

# Emergent competition resolves the paradox of stable microbial mutualisms

Oliver J. Meacock  \*<sup>1</sup> and Sara Mitri  <sup>2</sup>

<sup>1</sup>School of Biosciences, University of Sheffield, Sheffield, United Kingdom

<sup>2</sup>Department of Fundamental Microbiology, University of Lausanne, Lausanne, Switzerland

## Abstract

What is the role of cooperation in determining ecosystem structure? This question is central to ecology, yet remains controversial; cooperative mechanisms such as plant-insect pollination and microbe-microbe cross-feeding are widespread, but ecological theory suggests that cooperative communities should be unstable. Here, we resolve this apparent contradiction by deriving a precise and general mapping between mechanistic interaction models and the generalised Lotka-Volterra (gLV) equation. By avoiding the common assumption that environmental and population dynamics occur on different timescales, we obtain a framework that is built on the rate of change of growth rates, *i.e.* growth accelerations. We apply our findings to a model of an obligatory mutualism between auxotrophic bacteria and obtain a counter-intuitive result: increasing the strength of cooperative mechanisms by increasing amino acid production rates causes competition to become stronger in the corresponding gLV model. At the same time, effective intrinsic growth rates become increasingly positive. These coupled effects allow enhanced cross-feeding to increase overall population sizes while maintaining ecosystem stability. Finally, we provide mechanistic insights into the resulting coexistence outcomes by exploiting an exact correspondence between mechanistic models and Modern Coexistence Theory (MCT) revealed by our framework. Our findings show that cooperative and competitive interaction mechanisms do not necessarily translate into positive and negative interaction strengths in phenomenological models, highlighting the importance of mechanistic insights for developing a correct understanding of ecosystem structure.

---

\*o.meacock@sheffield.ac.uk

## 1 Introduction

Mutually-beneficial interactions between populations, or mutualisms, are central to the establishment and persistence of organisms in ecosystems across scales [1]. While originally studied in the context of relationships between macroscopic organisms such as plants and their pollinators or cleaner fish and their clients, mutualistic relationships are now known to be fundamental to the composition of many microbial ecosystems [2]. In the most extreme cases, isolates initially identified as pure cultures of single species have been unmasked as assemblies of mutually-dependent bacteria upon closer examination [3, 4]. More broadly, auxotrophic microbes that lack the ability to synthesise essential vitamins, amino acids and/or nucleotides are widespread in the environment and human-associated microbiomes [5–7]. Such metabolic deficiencies must be compensated for by secretions from surrounding organisms to allow auxotrophic species to persist. The diversity and function of microbiomes is thus strongly influenced by nutritional exchanges [2, 8, 9].

Surprisingly, despite these widespread observations of mutualisms in nature, theoretical investigations based on the generalised Lotka-Volterra (gLV) framework and related models suggest that mutualisms should destabilise ecosystems [10–12]. Reconciling these apparently contradictory results has been a pressing challenge for theoretical ecologists in recent decades [13–17]. While introducing more realistic representations of the underlying biological processes mediating interactions can enhance the stability of mutualisms [18–21], these modifications remain largely *ad hoc* as they are not derived from an explicit mechanistic representation of the system. Instead, they are based on intuitive but untested assumptions of how changes to interaction mechanisms should impact interaction values.

There is a fundamental technical barrier to resolving this problem using theory: while we can explicitly represent the mechanisms that mediate mutualisms (e.g. nutritional exchanges [22–24]) relatively straightforwardly, we have thus far been unable to identify a generic mapping between these mechanistic models and phenomenological interaction frameworks such as the gLV model. Achieving such a mapping is a long sought-after goal in theoretical ecology, first attempted by MacArthur in his pioneering work on resource competition [25]. However, despite decades of efforts to understand the connections between these two frameworks [24, 26–30], a general formulation for identifying equivalencies between the two remains elusive. Several studies have highlighted fundamental differences between their predictions and structures,

58 suggesting that a direct correspondence may not exist [31–33].

59 In this work, we resolve this challenge by deriving a general and precise mapping between  
60 mechanistic and phenomenological interaction frameworks that is based on growth accelera-  
61 tions rather than rates. Conveniently, our results allow us to directly apply much of the theoret-  
62 ical toolset built to study the gLV equation to mechanistic interaction models. By applying these  
63 tools to a two-population model of cross-feeding auxotrophic bacteria, we show that manipulat-  
64 ing mechanistic parameters can result in counter-intuitive effects on effective gLV parameters.  
65 Specifically, we show that increasing the production rate of cross-fed compounds paradoxically  
66 increases effective competition between mutualists. This effect emerges because cross-fed  
67 nutrients become less growth limiting as their production is increased. Consequently, growth  
68 limitation imposed by non cross-fed resources that are consumed by both mutualists becomes  
69 more dominant. Changes in coexistence outcomes resulting from these mechanistic changes  
70 can be exactly captured by applying Modern Coexistence Theory (MCT) through our framework,  
71 with stronger cross-feeding exchanges increasing niche overlap. Our findings thus provide an  
72 unexpected explanation for the stability of microbial mutualisms that is rooted in an under-  
73 standing of interaction mechanisms.

## 74 **2 Results**

### 75 **2.1 A generic mapping between mechanistic and phenomenological interaction** 76 **frameworks**

77 In phenomenological frameworks such as the gLV model, growth rates are shaped purely by the  
78 population densities (Fig. 1a). The gLV model treats interaction strength as a linear function of  
79 partner density on a focal populations' per-capita growth rate (PCGR, defined as  $\frac{1}{x_\alpha} \frac{dx_\alpha}{dt}$ ):

$$\frac{1}{x_\alpha} \frac{dx_\alpha}{dt} = \mu_\alpha + \sum_{\beta} a_{\alpha\beta} x_\beta. \quad (1)$$

80 Here,  $x_\alpha$  is the instantaneous density of focal population  $\alpha$ ,  $\mu_\alpha$  is the 'intrinsic growth rate' of  
81  $\alpha$  (its growth rate at low densities and in the absence of other populations) and  $a_{\alpha\beta}$  are the  
82 interaction strengths (the growth rate impact of one unit of population  $\beta$  on  $\alpha$ ). These can be  
83 assembled into a matrix of values  $A$  called the interaction matrix [34]. The equilibrium solution

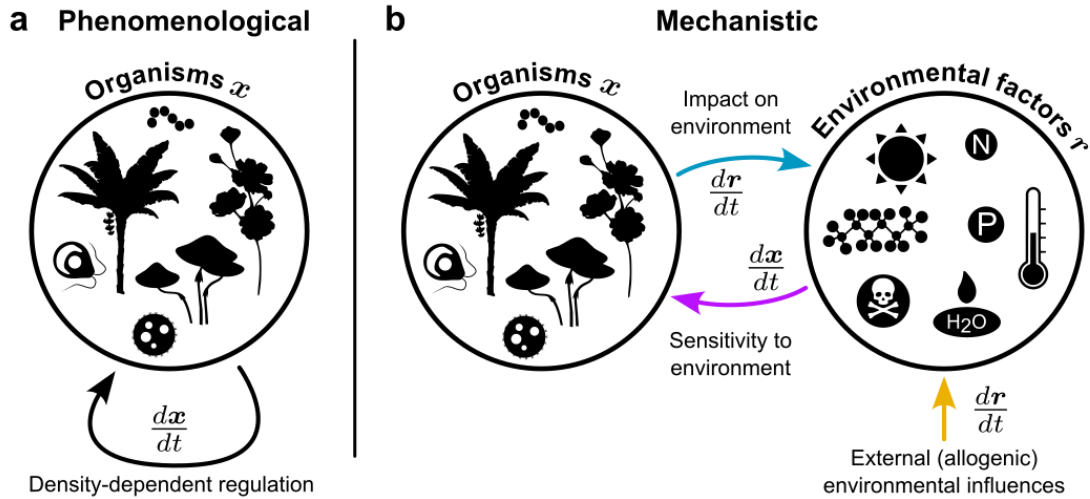


Figure 1: **Structures of phenomenological and mechanistic ecosystem models.** Colours of arrows in panel b correspond to the colour scheme used throughout this manuscript for impact functions (blue), sensitivity functions (purple) and allogenic functions (gold).

84 to such a system is called ‘feasible’ if the equilibrium densities (given by  $x^* = -\mu A^{-1}$ ) are  
 85 strictly positive.

86 Alternatively, interaction mechanisms can be explicitly represented by splitting the ecosystem  
 87 into two groups of dynamical quantities: the sizes of the populations of interest  $x$  and the  
 88 quantities of environmental factors  $r$  that influence these populations’ growth rates (Fig. 1b).  
 89 Although often treated as the concentrations of abiotic environmental compounds in plant and  
 90 microbial community ecology [35, 36], these are more general and may also include factors  
 91 such as biotic resources that can self-replicate [25]. The key structural determinant of these  
 92 models is that they are bipartite:  $x$  can influence  $r$  and  $r$  can influence  $x$ , but there are no  
 93 direct relationships between different members of  $x$  or  $r$ .

94 The dynamics of the environmental factors are determined by a combination of impacts by the  
 95 community, which we represent with environment-dependent impact functions  $f_{\beta}(r)$  [30], and  
 96 extrinsic processes that are independent of the community (e.g. fluxes of compounds into the  
 97 ecosystem or reproduction of biotic resources) which we represent with the allogenic function  
 98  $\sigma(r)$ . Putting these together, we can then write the rate of change of the environmental factors  
 99  $r$  as:

$$\frac{dr}{dt} = \sum_{\beta} x_{\beta} f_{\beta}(r) + \sigma(r) \quad (2)$$

100 The *sensitivity function*  $g_\alpha$  describes the growth rate of a population  $\alpha$  in a particular environ-  
 101 ment:

$$\frac{1}{x_\alpha} \frac{dx_\alpha}{dt} = g_\alpha(\mathbf{r}). \quad (3)$$

102 While these are often described as the basic equations of consumer-resource models [37], we  
 103 refer to this class of system more generally as Environment-Organism (EO) models to emphasise  
 104 that environmental factors need not be resources and that population need not consume them  
 105 [36, 38]. The impact and sensitivity functions together encode the mechanisms through which  
 106 the populations  $x$  interact, and can be constructed to describe a very broad range of biological  
 107 processes (Table S1).

108 Identifying a general way to convert these expressions into a gLV-like equation (Eq. 1) is desir-  
 109 able as it would allow us to understand how underlying interaction mechanisms ultimately shape  
 110 coexistence. Current techniques for performing this mapping rely on approximations such as  
 111 the separation of timescales between environmental and population dynamics [24, 25, 30, 39]  
 112 or low population densities [29], or are applicable only to specially-selected EO systems with  
 113 convenient algebraic properties [26, 27, 35]. A common feature of most such approaches is  
 114 their adoption of a first order perspective, aiming to derive an expression that describes the  
 115 current growth rates in terms of the population densities as in the gLV equation. However, in-  
 116 teractions in mechanistic models result from the combination of two rate-based processes [40,  
 117 41]: the rate at which organisms impact the environment and the sensitivity of their growth rates  
 118 to environmental conditions. The combination of two first order processes might be expected  
 119 to lead to second order dynamics, *i.e.* growth accelerations.

120 Following this logic, we can evaluate the temporal derivative of the populations' PCGRs to obtain  
 121 the per-capita growth acceleration (PCGA,  $\frac{d}{dt} \left( \frac{1}{x_\alpha} \frac{dx_\alpha}{dt} \right)$ ):

$$\frac{d}{dt} \left( \frac{1}{x_\alpha} \frac{dx_\alpha}{dt} \right) = \nabla g_\alpha \cdot \frac{d\mathbf{r}}{dt}, \quad (4)$$

122 where we have used the multivariable chain rule to split the temporal derivative of the sensitivity  
 123 function into the sensitivity gradients with respect to the environmental factors ( $\nabla g_\alpha \equiv \frac{\partial g_\alpha}{\partial \mathbf{r}}$ )  
 124 and the rate of environmental change. Substituting in Eq. 2, we obtain (Supplementary Note

125 2.1):

$$\frac{d}{dt} \left( \frac{1}{x_\alpha} \frac{dx_\alpha}{dt} \right) = \mu'_\alpha(\mathbf{r}) + \sum_{\beta} a'_{\alpha\beta}(\mathbf{r}) x_\beta. \quad (5)$$

126 This equation, which we will refer to as the accelerational Environment-Organism (aEO) equa-  
127 tion, partitions the PCGA into two parts: the abiotic acceleration  $\mu'_\alpha(\mathbf{r}) \equiv \boldsymbol{\sigma}(\mathbf{r}) \cdot \nabla g_\alpha(\mathbf{r})$  repre-  
128 sents the rate of change of the growth rate of  $\alpha$  due to the extrinsic drivers of the environmental  
129 factors, while the term  $\sum_{\beta} a'_{\alpha\beta}(\mathbf{r}) x_\beta$  captures the growth rate impacts caused by the commu-  
130 nity's impact on the environmental factors. Central to this term are the biotic accelerations  
131  $a'_{\alpha\beta}(\mathbf{r}) \equiv \mathbf{f}_\beta(\mathbf{r}) \cdot \nabla g_\alpha(\mathbf{r})$ , which capture the per-capita contribution to this effect from each  
132 community member.

133 Despite the fact that the gLV equation is first order and the aEO equation is second order, there  
134 are deep equivalencies between the two. Notably, at an equilibrium state in environment  $\mathbf{r}^*$ ,  
135  $\frac{d}{dt} \left( \frac{1}{x_\alpha} \frac{dx_\alpha}{dt} \right) = 0$ . We therefore obtain

$$0 = \mu'_\alpha(\mathbf{r}^*) + \sum_{\beta} a'_{\alpha\beta}(\mathbf{r}^*) x_\beta, \quad (6)$$

136 *i.e.* an expression that is algebraically identical to the gLV equation (Eq. 1) at equilibrium. This  
137 result means that for many rate-based mathematical statements which are true for an equilib-  
138 rium gLV system, there is a parallel acceleration-based statement which holds for all equilib-  
139 rium EO systems. We discuss some of the tools that can be built through this parallelism in  
140 Supplementary Note 2.3. This result is exact and general, only requiring that  $g_\alpha(\mathbf{r})$  is differ-  
141 entiable with respect to the environmental factors, such that the sensitivity gradient  $\nabla g_\alpha(\mathbf{r})$  is  
142 well-defined.

## 143 **2.2 A simulated cross-feeding community demonstrates counter-intuitive re-** 144 **lationships between interaction mechanisms and effective gLV parame-** 145 **ters**

146 To illustrate how these results inform our understanding of mutualistic exchanges in microbial  
147 ecosystems, we built a two-population EO model representing obligate cross-feeding between  
148 two auxotrophic bacterial populations,  $\hat{v}$  and  $\hat{w}$ , which require external supplies of amino acids

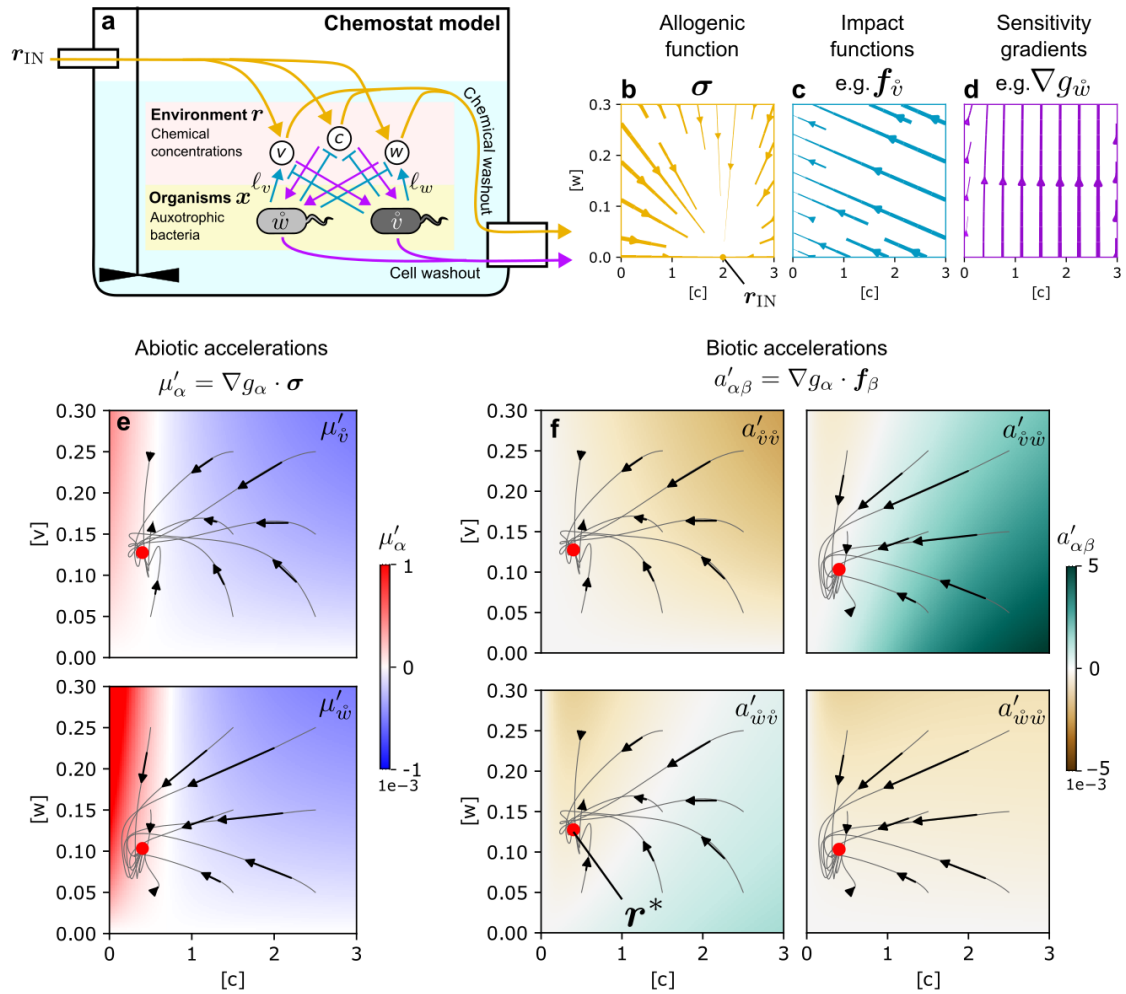


**Figure 2: An accelerational description of cross-feeding auxotrophs at equilibrium.** EO models consist of three components – allogenic functions, sensitivities and impacts – that together represent the mechanisms through which organisms interact. a) We built an EO model representing a community of two cross-feeding auxotrophic bacteria (each unable to synthesise one of two amino acids  $v$  and  $w$ ) in a chemostat. Metabolic dependencies on a carbon source  $c$  and amino acids are encoded by sensitivity functions (purple), while consumption and production are represented by impact functions (blue, arrows indicate production, bars consumption). These functions are constructed using explicit mechanistic parameters such as the amino acid production rates  $l_v$  and  $l_w$ . Allogenic processes in this system (gold) are the external influences on chemical concentrations, *i.e.* nutrient influx and washout of chemicals through the chemostat efflux. Washout of cells at the same rate also acts as an effective mortality term. b-d) These three processes can be represented as vector fields in the ‘environment space’, the space of possible environmental compositions  $r$ . e,f) Taking the scalar product of the sensitivity gradients and allogenic processes yields the abiotic accelerations (e), while the scalar product of the sensitivity gradients and impact functions yields the biotic accelerations (f). These can be represented as scalar fields sitting in the environment space. The chemical environment converges on an equilibrium composition  $r^*$  (red circle) regardless of the starting composition of the media in the chemostat (grey trajectories and arrows). Note that the full environment space is three dimensional, representing the concentrations of  $c, v$  and  $w$  (Fig. S2). In b-d, we display slices through this space for which the concentration of the chemical corresponding to the suppressed axis is set to zero. Environmental trajectories (c,d) are projected onto this plane. Arrow thickness in b indicates the local magnitude of the vector field. Dilution rate  $D = 0.01$ .

149  $v$  and  $w$  respectively. This type of system is a popular choice for studying mutualisms in the  
 150 lab [23, 42–46] and is widely observed in environmental microbiomes [2, 4, 6]. Our formulation  
 151 (Methods) assumes that growth depends on co-utilisation of a carbon source  $c$  (used by both  
 152 partners) and a population-specific amino acid ( $v$  or  $w$ ) that is secreted by the mutualistic part-  
 153 ner. We also include ‘overflow’ production of amino acids when an auxotroph’s essential amino  
 154 acid is at low concentrations but the concentration of the carbon source is high, reflecting re-  
 155 cent experimental findings [47] (Fig. 2a). This community was then placed into a simulated  
 156 chemostat, an idealised representation of systems with continual inflows and outflows of ma-  
 157 terial such as the gut [48]. In the absence of external amino acids, this model has multiple  
 158 features of obligatory mutualisms including bistability and Allee effects [20] (Fig. S1).

159 The mechanistic processes that define an EO model can be represented as vector fields sitting  
 160 in the ‘environment space’, which represents all possible combinations of the environmental  
 161 factors (Figs. 2b-d, S2). The allogenic function and impact functions indicate the direction  
 162 that the environment is pulled by the abiotic and biotic influences on the environment, respec-  
 163 tively. For example, dilution of a chemostat’s content with media of composition  $r_{\text{IN}}$  results in  
 164 an allogenic function in which all vectors point towards  $r_{\text{IN}}$  (Fig. 2b). Sensitivity gradients can  
 165 also be represented as vector fields, now representing the rate at which a population’s growth  
 166 rate changes as the environment is pulled in a given direction (Fig. 2d). Taking scalar prod-  
 167 ucts of these vector fields give scalar fields that represent the rate at which the growth rate  
 168 of population  $\alpha$  is modified by the external drivers of the environmental dynamics (the abiotic  
 169 acceleration,  $\mu'_{\alpha}(\mathbf{r})$ ) or by the effect of another community member  $\beta$  on the environment (the  
 170 biotic accelerations,  $a'_{\alpha\beta}(\mathbf{r})$ ).

171 While  $\mu'_{\alpha}(\mathbf{r})$  and  $a'_{\alpha\beta}(\mathbf{r})$  can change as environmental conditions fluctuate [36] (Fig. S3), we  
 172 will generally focus on their values in an equilibrium environment  $\mathbf{r}^*$ , *i.e.*  $a'_{\alpha\beta}(\mathbf{r}^*)$  and  $\mu'_{\alpha}(\mathbf{r}^*)$   
 173 (Fig. 2c,d). Under these conditions, they can be treated as effective gLV parameters through  
 174 the algebraic correspondence between Eqs. 6 and 1. Beyond this point, we will suppress the  
 175 explicit dependency on  $\mathbf{r}^*$  for notational compactness.

176 In previous studies, the stability of such two-population mutualisms has been investigated  
 177 through modified gLV equations that introduce new quantities – for example, terms that cause  
 178 facilitation to saturate or become competitive as the donor’s density increases [21, 49]. These  
 179 modifying terms are, in effect, intended to impose non-linear density-dependencies on top of

180 the linear density-dependencies of the Lotka-Volterra model that more realistically represent  
181 the mechanisms underpinning the mutualism. However, as interaction mechanisms are not  
182 explicitly represented in such models, the proposed relationship between mechanisms and ef-  
183 fective gLV parameters remains a choice that must be intuited by the modeller. By contrast,  
184 the mechanistically explicit mapping between Eqs. 1 and 6 allows us to avoid this intuitive leap.  
185 How does this affect our understanding of the stability of mutualisms?

186 To investigate this question, we asked how the biotic accelerations  $a'_{\alpha\beta}$  and abiotic accelera-  
187 tions  $\mu'_\alpha$  (which are algebraically homologous to interaction strengths  $a_{\alpha\beta}$  and intrinsic growth  
188 rates  $\mu_\alpha$  respectively) vary as the amino acid production rate  $\ell_w$  is increased, representing an  
189 evolutionary scenario in which one population unilaterally modifies its cross-feeding strategy  
190 [50]. From a naïve interpretation of the gLV model, we would expect this to result in stronger  
191 positive interactions from the producer to the consumer, while the costs associated with amino  
192 acid production would drive increasingly negative intrinsic growth rates for the producer [10,  
193 20].

194 To test whether this prediction held in our mechanistic model, we allowed the simulated chemo-  
195 stat to reach an equilibrium for each value of  $\ell_w$  and recorded the equilibrium densities of  $\hat{v}$   
196 and  $\hat{w}$  (Fig. S4a, lines), biotic accelerations  $a'_{\hat{v}\hat{v}}$ ,  $a'_{\hat{v}\hat{w}}$ ,  $a'_{\hat{w}\hat{w}}$  and  $a'_{\hat{w}\hat{v}}$  (Fig. 3a) and abiotic accel-  
197 erations  $\mu'_{\hat{v}}$  and  $\mu'_{\hat{w}}$  (Fig. 3b). Surprisingly, while the biotic accelerations were initially positive,  
198 they switched signs to negative as the strength of the cooperative mechanism was increased.  
199 By contrast, the abiotic accelerations grew in value, becoming increasingly positive after being  
200 negative at low production rates. While these relationships were unexpected, the accelerational  
201 analogue of the expression relating equilibrium densities to gLV parameters ( $x^* = -\mu' A'^{-1}$ )  
202 accurately yielded the equilibrium densities  $x^*$  (Fig. S4a, circles), confirming the algebraic cor-  
203 respondence between Eqs. 1 and 6. We also found that the real part of the system's eigenvalue  
204 spectrum was negative for all production values (Supplementary Note 2.3.2, Fig. S5), indicating  
205 linear stability of coexistence (Fig. S4b). These results are not an artefact of the small size of  
206 the community or the choice of mechanistic parameters, as they generalise to larger commu-  
207 nities with random parameters [51] (Fig. S6). This suggests that our intuitive understanding  
208 of the relationship between interaction mechanisms and effective gLV parameters is flawed:  
209 increased cross-feeding leads to stronger mutual growth but also stronger competition.

210 To gain a deeper understanding of the processes driving this paradoxical relationship, we turned

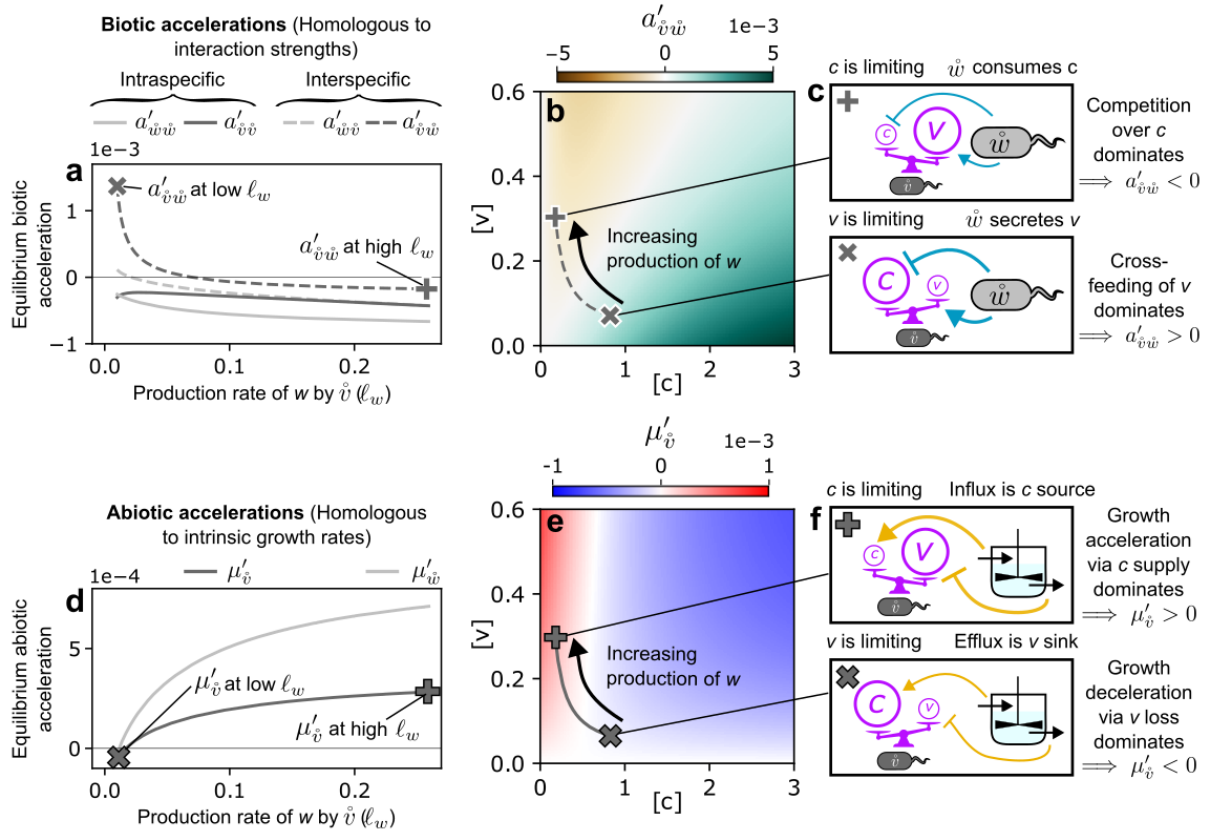


**Figure 3: Modulation of auxotroph amino acid production rates causes counter-intuitive changes to effective gLV parameters.** a,d) Keeping all other parameters fixed, we varied the rate at which  $\bar{v}$  converts the carbon source to secreted  $w$ ,  $\ell_w$ , and numerically simulated each chemostat's dynamics until it reached an equilibrium. We then evaluated the equilibrium biotic accelerations for each pair of populations (a) and abiotic accelerations for each population (d). b,e) Counter-intuitive relationships between the varying strength of the cooperative cross-feeding mechanism and the effective gLV parameters can be understood by plotting the changing position of  $r^*$  on the scalar fields representing one of the biotic (b) and abiotic (e) accelerations (replotted from Fig. 2 e and f). c,f) Schematics representing the mechanisms driving changes in effective gLV parameters under different production rates of  $w$ .  $\times$  and  $+$  symbols represent simulations with the lowest and highest production rates of  $w$ , respectively. Dilution rate  $D = 0.01$ .

211 to the scalar fields representing the inter-specific biotic acceleration  $a'_{\hat{v}\hat{w}}$  (Fig. 3b) and the  
 212 abiotic acceleration  $\mu'_{\hat{v}}$  (Fig. 3e). We selected these over  $a'_{\hat{w}\hat{v}}$  and  $\mu'_{\hat{w}}$  as they are independent  
 213 of  $\ell_w$  and thus remain fixed over the parameter sweep. As the production of  $w$  increases, the  
 214 equilibrium concentration of  $c$  decreases while the concentration of  $v$  increases, driven by the  
 215 increased density of the  $w$  auxotroph. In the low production scenario, the concentration of  
 216 the amino acid is growth limiting and cross-feeding of  $v$  from  $\hat{w}$  dominates over competition  
 217 for carbon, leading to a positive net value of  $a'_{\hat{v}\hat{w}}$ . By contrast, carbon limitation in the high  
 218 production scenario leads to dominance of carbon-based competition between the two strains,  
 219 creating a negative net value (Fig. 3c). A similar argument applies to the abiotic accelerations,  
 220 but with the effect of the external processes (*i.e.* the fluxes of chemicals into and out of the  
 221 chemostat) substituted in place of the mutualistic partner; domination of loss of amino acids  
 222 through the system's efflux drives a negative net value of  $\mu'_{\hat{v}}$  in the amino-acid limited low  
 223 production scenario, while the positive growth rate impact of the carbon supply dominates in  
 224 the carbon-limited high production scenario (Fig. 3f).

### 225 **2.3 How nutrient exchanges shape coexistence: mapping mechanisms to MCT**

226 With a clearer understanding of the relationship between mutualistic mechanisms and effective  
 227 gLV parameters, we are now equipped to move one level higher and understand how mecha-  
 228 nisms shape coexistence. Two-population ecosystems have been extensively studied through  
 229 the lens of Modern Coexistence Theory (MCT), which seeks to partition processes that impact  
 230 coexistence outcomes into stabilising components that reduce the niche overlap between pop-  
 231 ulations and equalising components that balance the fitness ratio between populations [28]. A  
 232 classic result arising from two-population Lotka-Volterra models is that explicit expressions for  
 233 the niche overlap  $\rho$  and fitness ratio  $\frac{k_1}{k_2}$  can be obtained from the gLV parameters (Supplemen-  
 234 tary Note 2.3.3) [52, 53]:

$$\rho = \sqrt{\frac{a_{12}a_{21}}{a_{11}a_{22}}} \quad (7a)$$

$$\frac{k_1}{k_2} = \frac{\mu_1}{\mu_2} \sqrt{\frac{a_{22}a_{21}}{a_{11}a_{12}}} \quad (7b)$$

235 where 1 and 2 are labels for the two populations. Coexistence is feasible only if

$$\rho < \frac{k_1}{k_2} < \frac{1}{\rho}. \quad (8)$$

236 We can define an accelerational analogue of this expression. Using the labels of the auxotrophs,  
237 we obtain:

$$\rho' = \sqrt{\frac{a'_{\hat{v}\hat{w}} a'_{\hat{w}\hat{v}}}{a'_{\hat{w}\hat{w}} a'_{\hat{v}\hat{v}}}} \quad (9a)$$

$$\frac{k'_{\hat{w}}}{k'_{\hat{v}}} = \frac{\mu'_{\hat{w}}}{\mu'_{\hat{v}}} \sqrt{\frac{a'_{\hat{v}\hat{v}} a'_{\hat{v}\hat{w}}}{a'_{\hat{w}\hat{w}} a'_{\hat{w}\hat{v}}}}. \quad (9b)$$

238 Mutualisms have previously been thought to be incompatible with this form of MCT, as positive  
239 intraspecific interaction strengths lead to imaginary niche overlaps [54]. However, we have  
240 already shown that values of  $a'_{\alpha\beta}$  are negative for most amino acid production rates, suggesting  
241 that we may be able to use this framework to analyse many instances of the cross-feeding  
242 system.

243 To test whether we could use this approach to shed light on the mechanistic basis of coexis-  
244 tence in this system, we manipulated the amino acids through two mechanisms: varying their  
245 concentrations in the input media  $r_{\text{IN}}$  (Fig. 4a-c) and varying their production rates by the two  
246 populations (Fig. 4d-f). We then scored communities based on whether one, both or neither  
247 population was able to persist at equilibrium (Fig. 4b,e). Finally, we mapped these scenarios  
248 onto niche overlap and fitness ratio axes using Eq. 9b to verify the accuracy of the coexistence  
249 predictions by MCT (Fig. 4c,f). Some communities displayed positive biotic accelerations,  
250 which were excluded from the niche overlap and fitness ratio calculations to avoid imaginary  
251 values. These tended to be located at the edges of the coexistence regions where amino acid  
252 concentrations were particularly limiting. For the remaining communities, we found that Eq. 9b  
253 precisely predicts the coexistence properties of this system, with combinations of mechanistic  
254 parameters that result in competitive exclusion mapped to the boundaries of the coexistence  
255 region.

256 How do coexistence outcomes change as underlying mechanisms are varied? Changes in the  
257 ratio of the input amino acid concentrations  $[v]_{\text{IN}}:[w]_{\text{IN}}$  (Fig. 4b,c, dashed line with black arrow-

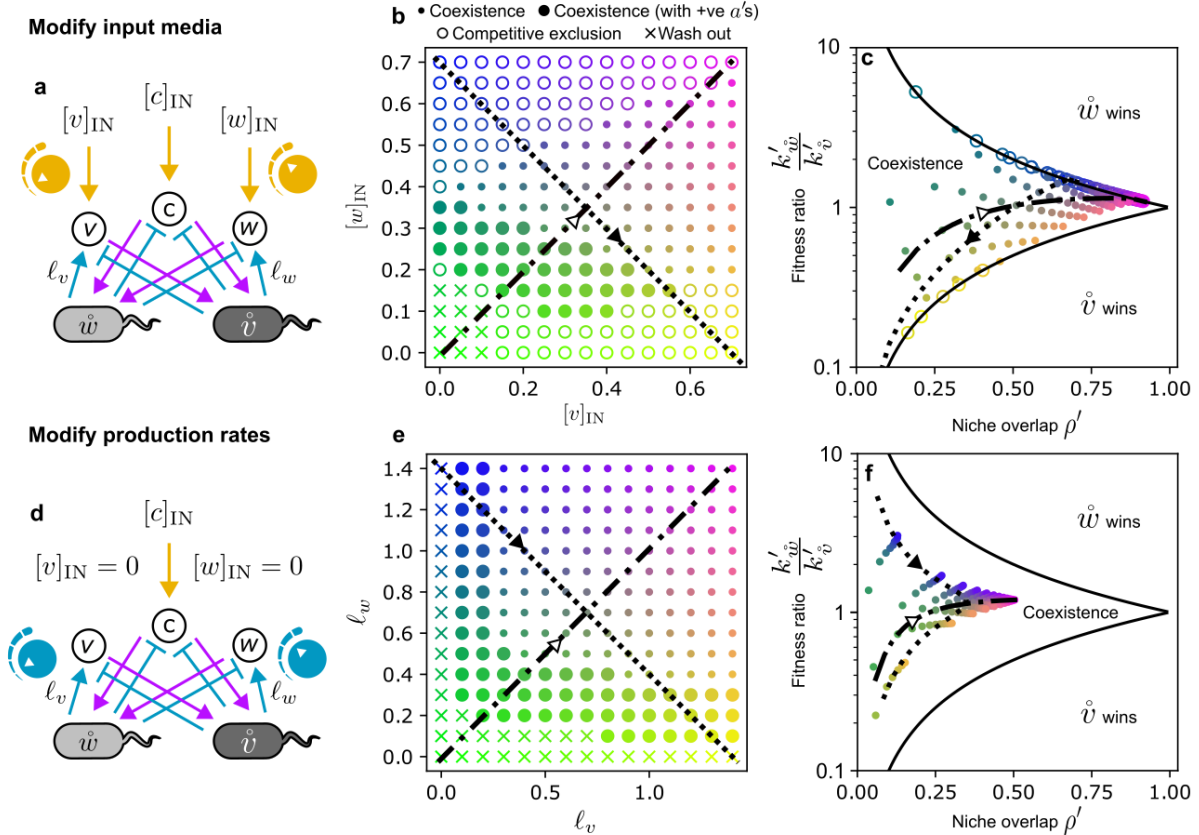


Figure 4: **Mapping interaction mechanisms onto modern coexistence theory** a) To test the validity of our accelerational definition of the niche overlap and fitness ratio, we first varied the input concentrations of the two amino acids in the two population auxotrophy model. b) We then performed numerical simulations of the population dynamics in the chemostat for each combination of input concentrations, scoring coexistence outcomes based on whether both populations were washed out (crosses), one population competitively excluded the other (open circles) or both populations stably coexisted (filled circles). c) The abiotic and biotic accelerations for both strains in the equilibrium environment  $r^*$  were then converted to niche overlaps  $\rho'$  and fitness ratios  $\frac{k'_{\hat{w}}}{k'_{\hat{v}}}$  (main text). Solid lines indicate predicted coexistence boundaries (Eq. 8). Note that the contours of constant input amino acid ratio (dot-dash line) and total input amino acid concentration (dotted line) are mapped onto the niche overlap and fitness ratio axes. d-f) Equivalent analysis conducted with varying amino acid production rates from the two auxotrophs. Large filled circles in b and e denote stably coexisting communities with at least one positive biotic acceleration  $a'$ , which are excluded from the niche overlap and fitness ratio axes in c and f. Simulations resulting in mutual wash out are also excluded from these axes. Points with matching colours in b, c and e, f correspond to the same simulation in the two panels. Dilution rate  $D = 0.03$ , input media contains no amino acids in d-f.

258 head) predominantly drove changes in fitness ratios, with the less supported population being  
259 outcompeted as soon as the system hit a coexistence boundary. On the other hand, increasing  
260 the total amino acid concentration while keeping their ratio fixed (Fig. 4b,c, dot-dashed line  
261 with white arrowhead) mainly changed the niche overlap, leading to a progression from mu-  
262 tual wash-out to coexistence and finally competitive exclusion as observed in experiments [23].  
263 A similar analysis on amino acid production rates (Fig. 4e,f) yielded closely related patterns.  
264 However, we found that no combination of production rates resulted in competitive exclusion,  
265 reflecting their mutual dependence in media lacking amino acids. Instead, correlated changes  
266 in the niche overlap and fitness ratio prevented the system from hitting the coexistence bound-  
267 ary (Fig. 4f).

268 We now investigated the mechanistic basis for these patterns. Adopting a sampling-based ap-  
269 proach, we generated communities with randomised amino acid production rates and input  
270 concentrations and scored the fitness ratio and niche overlap of each pair of strains at equi-  
271 librium. We then binned communities according to their values of these two quantities and  
272 calculated the average nutrient concentrations, mechanistic parameters (Fig. 5a-g) and effec-  
273 tive gLV parameters (Fig. S7) for all systems falling within these bins. This allowed us to relate  
274 variations in the MCT metrics to underlying mechanistic processes (Fig. 5f): at low amino acid  
275 concentrations, the two populations are not competing for the carbon source as their growth  
276 is limited by different amino acids. Processes that increase amino acid concentrations relieve  
277 this non-competitive growth constraint and instead shift the populations towards competition  
278 for the carbon source on which they are mutually dependent, driving an increase in niche over-  
279 lap (Fig. 5a-c). Fitness ratios on the other hand are determined by the relative fluxes of the two  
280 amino acids, with imbalanced fluxes favouring the auxotroph receiving the stronger supply of  
281 their limiting nutrient (Fig. 5d-g).

282 This perspective also allows us to explain why the system responds differently when the imbal-  
283 ance in fluxes arises due to internal (production rates) versus external (input concentrations)  
284 changes in mechanisms. Similar to Song *et al.* [55], we find that mechanistic changes are not  
285 purely stabilising nor equalising. Introducing an imbalance in production rates leads to an im-  
286 balance in the fitness ratio. However, it also leads to weaker overall growth due to the mutual  
287 dependence of the populations. This in turn leads to lower niche overlap due to less competition  
288 for carbon, allowing coexistence to be maintained (dotted line in Fig. 4f). Similar patterns have

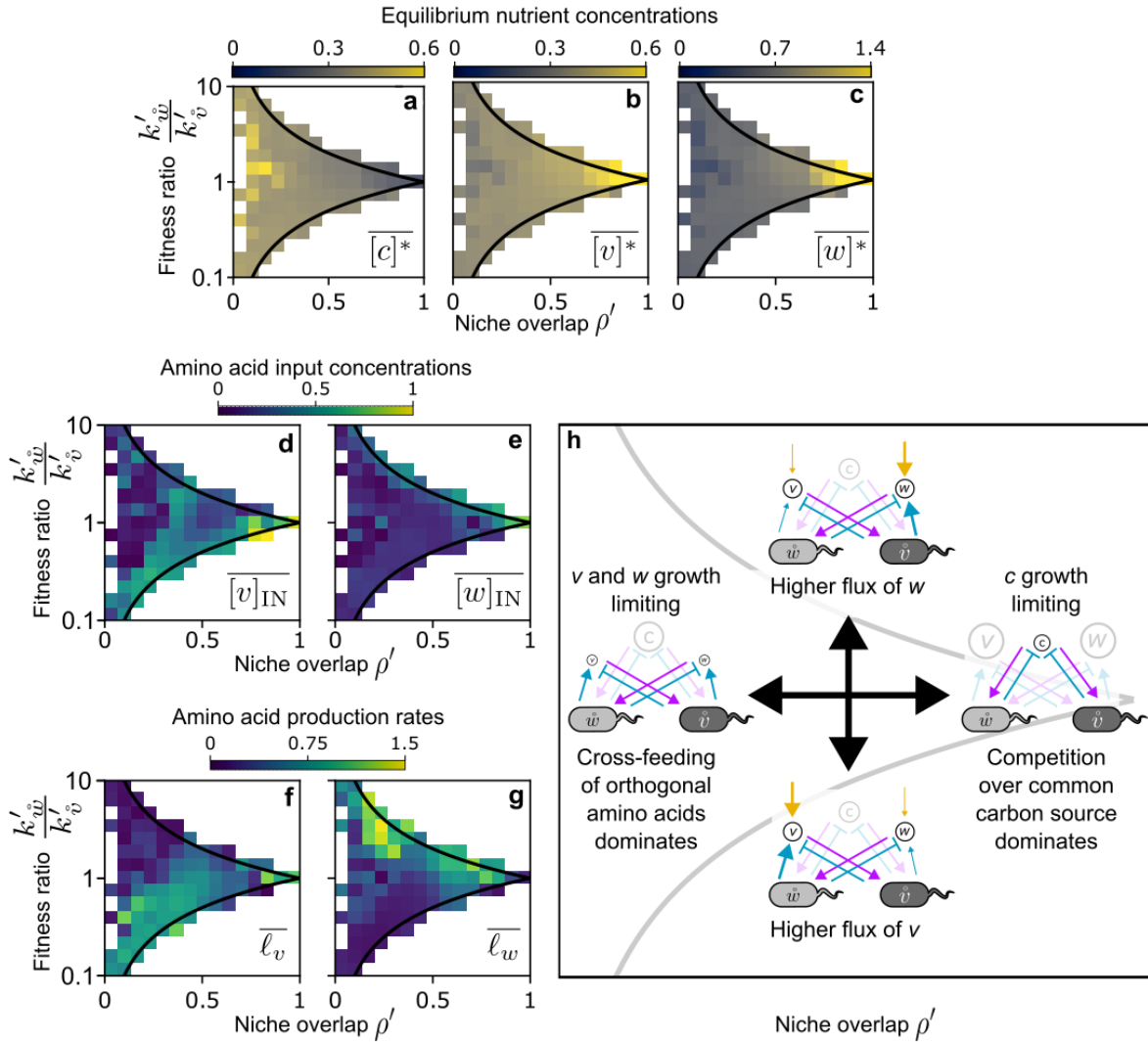


Figure 5: **The mechanistic basis of fitness ratios and niche overlaps of auxotrophic bacteria.** a-g) We generated communities with randomised combinations of amino acid production rates and amino acid input concentrations and evaluated the niche overlap  $\rho'$  and fitness ratio  $\frac{k'_{vw}}{k'_v}$  for each community at equilibrium. We then binned communities along these axes and calculated the average equilibrium carbon source concentration  $[c]^*$  (a) and amino acid concentrations  $[v]^*$ ,  $[w]^*$  (b,c), as well as the amino acid input concentrations  $[v]_{IN}$ ,  $[w]_{IN}$  (d,e) and production rates  $\bar{l}_v$ ,  $\bar{l}_w$  (f,g) for all communities falling within each bin. h) Summary of mechanisms driving changes in niche overlap and fitness ratios in the auxotrophy model. As in Fig. 4, communities with positive biotic accelerations were excluded from the analysis. Dilution rate  $D = 0.03$ .

289 been observed experimentally, with increased production of an amino acid by one member of  
290 a cross-feeding mutualism favouring the recipient but never leading to competitive exclusion  
291 [46]. On the other hand, imbalances in externally supplied amino acid concentrations are not  
292 subject to this internal regulation through changes in niche overlap. This allows imbalances  
293 in the fitness ratio to drive the system into the coexistence boundary, enabling competitive  
294 exclusion (dotted line in Fig. 4c).

### 295 **3 Discussion**

296 The relative roles of cooperation versus competition in ecosystems is a long-debated topic  
297 in ecology [14–16, 56–58]. Within microbiology, this controversy is perhaps best reflected in  
298 the apparently contradictory results of studies that measure interaction strengths, which are  
299 predominantly competitive [59], versus those that study interaction mechanisms, which find  
300 widespread mutualistic exchanges [2]. Our results reconcile these two camps by showing that  
301 the term ‘mutualism’ means two different things, depending on the ecosystem property being  
302 investigated. The auxotrophy system that we model here is a paradigmatic obligate mutualism  
303 in terms of the ability of the two strains to persist (Fig. S1). Yet when we look at the quantities  
304 algebraically equivalent to the interaction strengths of the gLV model  $a_{\alpha\beta}$ , the biotic accelera-  
305 tions  $a'_{\alpha\beta}$ , we observe that competition dominates and becomes stronger as cross-feeding is  
306 strengthened (Fig. 3). This is generally expected to stabilise communities [11, 12]. Cross-feeding  
307 communities can thus be mutualistic in terms of their persistence properties, but competitive  
308 as far as their stability is concerned.

309 In line with these results, previous studies have shown that the restraining effect of competi-  
310 tion over shared resources can prevent mutualisms from destabilising ecosystems. Aside from  
311 carbon availability, these limiting factors can include nitrogen, space and the density of shared  
312 partners [11, 33, 45, 60]. Similar arguments have also been made for groups of macroscopic  
313 organisms, such as complexes of Müllerian mimics that compete for nectar [61]. However, an  
314 important outstanding question in the context of gLV-type models is why this enhanced compe-  
315 tition does not also suppress population sizes. Our results show that increased competition is  
316 compensated for by a paradoxical increase in the term that plays the role of the intrinsic growth  
317 rates  $\mu_\alpha$ , the abiotic accelerations  $\mu'_\alpha$  (Fig. 3). This finding contrasts with the typical assump-  
318 tion that  $\mu_\alpha$  is either fixed or declines with increasing costs of cooperation, demonstrating that

319 though algebraically equivalent at equilibrium, the gLV and aEO equations have fundamentally  
320 different interpretations. Indeed, there is nothing ‘intrinsic’ about  $\mu'_{\alpha}$ , which is largely deter-  
321 mined by the extrinsic environmental inputs. Studies which assume that intuitive relationships  
322 hold between interaction mechanisms and effective gLV parameters should be revisited in light  
323 of this alternative interpretation.

324 These findings also impact our understanding of the niche overlap and fitness ratio metrics of  
325 MCT. While our results are consistent with previous geometric interpretations of niche overlap  
326 as the degree of alignment between requirements or impacts of populations [27, 29, 52], our  
327 interpretation of the fitness ratio is more difficult to reconcile with existing work; certainly it  
328 is not obvious how to interpret the observed relationships as variations in fitnesses. While  
329 our findings suggest that it represents the extent to which fluxes of environmental quantities  
330 favour a particular population (Fig. 5h), additional EO models should be interrogated to assess  
331 the universality of this interpretation. Regardless of their interpretation however, the ability to  
332 map mechanistic processes onto the metrics of MCT represents a powerful simplification of  
333 ecosystems, allowing us to distil ecosystem processes involving an almost unlimited number of  
334 environmental factors down to two numbers that completely determine coexistence [62].

335 The main technical advance of our work is the derivation of a general and exact method for trans-  
336 forming mechanistic ecosystem models into a gLV-like parametrisation, allowing tools used to  
337 analyse gLV systems to be applied to mechanistic models. MacArthur’s solution to this prob-  
338 lem, based on the assumption that resources equilibrate much more rapidly than populations  
339 [25], has dominated the literature since its discovery [52, 55, 63–65]. However, this technique  
340 is approximate and can only be applied in cases where the dynamics of resources are logistic  
341 [26], a serious limitation when modelling the dynamics of ecosystems based on abiotic nutrients  
342 such as microbiota. Our approach avoids eliminating this timescale of the resource dynamics,  
343 consequently resulting in a second-order description of the population dynamics. It remains to  
344 be seen whether this accelerational picture proves a more accurate description of real ecosys-  
345 tems than existing rate-based representations, although we note that changes in population  
346 growth rates (*i.e.* growth accelerations) in closed microcosms are accurately described by a  
347 limiting case of the aEO equation [36]. Second-order descriptions also enable replication of  
348 phenomena not observed in standard first-order systems, such as density oscillations of single  
349 populations and time lags in population responses [66–68].

350 Our results also suggest new solutions to practical problems in microbial ecology. Currently,  
351 extensive measurements of environmental quantities are required to couple mechanistic mod-  
352 els to experiments, significantly limiting their utility [69]. On the other hand, the gLV model is  
353 unable to capture ecosystems governed by indirect interaction mechanisms, and must be made  
354 substantially more complex through terms representing higher order interactions (HOIs) [32].  
355 Remarkably, Eq. 6 resolves both of these problems: while it takes the environmentally-mediated  
356 interaction structure of microbial communities into account, it contains only single-species and  
357 pairwise terms which can be determined without explicit environmental measurements. By com-  
358 bining the advantages of the mechanistic and phenomenological viewpoints, this insight may  
359 provide new approaches to the characterisation and control of microbial ecosystems.

360 However, our approach also has its drawbacks. One of the main attractions of the gLV model  
361 and related frameworks are their analytical tractability, forming the basis of a large body of  
362 results based on random matrix theory [11, 12, 70]. These results describe the properties of  
363 very large communities provided that the associated parameters follow prescribed statistical  
364 patterns. By contrast, our approach relies heavily on numerical integration schemes to solve  
365 system dynamics and obtain equilibrial environments  $r^*$  for which Eq. 6 holds. While tech-  
366 niques exist for calculating  $r^*$  analytically for specific models (Supplementary Note 2.2), these  
367 generalise poorly and typically require explicit evaluation of matrix inverses. They also assume  
368 *a priori* that such a point exists and is an attractor, rather than the system dynamics converging  
369 on indefinite oscillations or chaos. Application of random matrix theory through this framework  
370 is therefore likely to be challenging.

371 In summary, our results provide a highly flexible link between the molecular mechanisms un-  
372 derpinning interactions and emergent coexistence outcomes. Application of this framework to  
373 the question of how interaction mechanisms constrain ecosystems promises to resolve a num-  
374 ber of outstanding problems in ecology beyond the paradox that we address here. Successfully  
375 addressing these problems will provide us with new tools for understanding and manipulating  
376 ecosystems across scales, including microbiomes.

## 377 **4 Acknowledgements**

378 We would like to thank Massimo Amicone, Simon van Vliet, Prajwal Padmanabha and Eric Ulrich  
379 for their valuable comments on a previous version of this manuscript, including terminological

380 suggestions by MA. We would also like to thank Vit Piskovsky, João Miranda, Ming Liu and es-  
381 pecially Prajwal Padmanabha for useful discussions on linear stability. OJM was supported by a  
382 Human Frontier Science Program (HFSP) long-term fellowship (LT0020/2022-L) and a Univer-  
383 sity of Sheffield Strategic Research Fellowship in the Physics of Life and Quantitative Biology.  
384 SM was supported by the National Center of Competence in Research Microbiomes grant SNF  
385 51NF40\_180575, Swiss National Science Foundation (SNSF) Eccellenza grant PCEGP3\_181272,  
386 and SNSF project grant 320030-236360.

## References

- 388 1. Bronstein, J. L. *Mutualism* en. Google-Books-ID: tIdCgAAQBAJ. ISBN: 978-0-19-967566-  
389 1 (Oxford University Press, 2015).
- 390 2. Kost, C., Patil, K. R., Friedman, J., Garcia, S. L. & Ralser, M. Metabolic exchanges are ubiqui-  
391 tuous in natural microbial communities. en. *Nature Microbiology* **8**. Publisher: Nature Pub-  
392 lishing Group, 2244–2252. ISSN: 2058-5276. [https://www.nature.com/articles/  
393 s41564-023-01511-x](https://www.nature.com/articles/s41564-023-01511-x) (2024) (Dec. 2023).
- 394 3. Bryant, M. P., Wolin, E. A., Wolin, M. J. & Wolfe, R. S. Methanobacillus omelianskii, a symbi-  
395 otic association of two species of bacteria. en. *Archiv für Mikrobiologie* **59**, 20–31. ISSN:  
396 1432-072X. <https://doi.org/10.1007/BF00406313> (2026) (Mar. 1967).
- 397 4. Morris, B. E., Henneberger, R., Huber, H. & Moissl-Eichinger, C. Microbial syntrophy: inter-  
398 action for the common good. *FEMS Microbiology Reviews* **37**, 384–406. ISSN: 0168-6445.  
399 <https://doi.org/10.1111/1574-6976.12019> (2026) (May 2013).
- 400 5. Gregor, R. et al. Vitamin auxotrophies shape microbial community assembly on model  
401 marine particles. *The ISME Journal* **19**, wraf184. ISSN: 1751-7362. [https://doi.org/10.  
402 1093/ismejo/wraf184](https://doi.org/10.1093/ismejo/wraf184) (2026) (Jan. 2025).
- 403 6. Yousif, G. et al. *Obligate cross-feeding of metabolites is common in soil microbial com-*  
404 *munities* en. Pages: 2025.01.29.635426 Section: New Results. Jan. 2025. [https://www.  
405 biorxiv.org/content/10.1101/2025.01.29.635426v1](https://www.biorxiv.org/content/10.1101/2025.01.29.635426v1) (2026).
- 406 7. Yu, J. S. et al. Microbial communities form rich extracellular metabolomes that foster  
407 metabolic interactions and promote drug tolerance. *Nature Microbiology* **7**. Publisher:  
408 Nature Publishing Group, 542–555. ISSN: 2058-5276. [https://www.nature.com/  
409 articles/s41564-022-01072-5](https://www.nature.com/articles/s41564-022-01072-5) (2023) (Mar. 2022).
- 410 8. Corral López, R. et al. Imbalance in gut microbial interactions as a marker of health and  
411 disease. *Science* **391**. Publisher: American Association for the Advancement of Science,  
412 890–895. <https://www.science.org/doi/full/10.1126/science.ady1729> (2026)  
413 (Feb. 2026).
- 414 9. Goldford, J. E. et al. Emergent simplicity in microbial community assembly. *Science* **361**.  
415 Publisher: American Association for the Advancement of Science, 469–474. ISSN: 10959203.  
416 <http://science.sciencemag.org/> (2021) (Aug. 2018).
- 417 10. Gause, G. F. & Witt, A. A. Behavior of Mixed Populations and the Problem of Natural Selec-  
418 tion. *The American Naturalist* **69**. Publisher: The University of Chicago Press, 596–609.  
419 ISSN: 0003-0147. <https://www.journals.uchicago.edu/doi/abs/10.1086/280628>  
420 (2026) (Nov. 1935).
- 421 11. Coyte, K. Z., Schluter, J. & Foster, K. R. The ecology of the microbiome: Networks, compe-  
422 tition, and stability. *Science* **350**. Publisher: American Association for the Advancement  
423 of Science, 663–666. ISSN: 10959203. [https://www.science.org/doi/10.1126/  
424 science.aad2602](https://www.science.org/doi/10.1126/science.aad2602) (2023) (Nov. 2015).
- 425 12. Allesina, S. & Tang, S. Stability criteria for complex ecosystems. *Nature* **483**. arXiv: 1105.2071  
426 Publisher: Nature Publishing Group, 205–208. ISSN: 1476-4687. [https://www.nature.  
427 com/articles/nature10832](https://www.nature.com/articles/nature10832) (2022) (Feb. 2012).
- 428 13. Holland, J. N., Ness, J. H. & BRONSTEIN, J. L. Mutualisms as Consumer-Resource. *Ecol-*  
429 *ogy of predator-prey interactions*. Publisher: Oxford University Press, 17. [https://books.  
430 google.com/books?hl=en&lr=&id=A4ORDAAAQBAJ&oi=fnd&pg=PA17&dq=info:  
431 ukF1bYyxCTsJ:scholar.google.com&ots=JfEI8xodZY&sig=TeTf8068dP4-axdyujVtg3oYuxQ](https://books.google.com/books?hl=en&lr=&id=A4ORDAAAQBAJ&oi=fnd&pg=PA17&dq=info:ukF1bYyxCTsJ:scholar.google.com&ots=JfEI8xodZY&sig=TeTf8068dP4-axdyujVtg3oYuxQ)  
432 (2026) (2005).
- 433 14. Rohr, R. P., Saavedra, S. & Bascompte, J. On the structural stability of mutualistic systems.  
434 *Science* **345**. Publisher: American Association for the Advancement of Science, 1253497.  
435 <https://www.science.org/doi/full/10.1126/science.1253497> (2026) (July 2014).
- 436 15. Jones, E. I., Bronstein, J. L. & Ferrière, R. The fundamental role of competition in the ecol-  
437 ogy and evolution of mutualisms. en. *Annals of the New York Academy of Sciences* **1256**.

- 438 \_eprint: <https://nyaspubs.onlinelibrary.wiley.com/doi/pdf/10.1111/j.1749-6632.2012.06552.x>,  
439 66–88. ISSN: 1749-6632. [https://onlinelibrary.wiley.com/doi/abs/10.1111/j.  
440 1749-6632.2012.06552.x](https://onlinelibrary.wiley.com/doi/abs/10.1111/j.1749-6632.2012.06552.x) (2026) (2012).
- 441 16. Bastolla, U. *et al.* The architecture of mutualistic networks minimizes competition and  
442 increases biodiversity. en. *Nature* **458**. Publisher: Nature Publishing Group, 1018–1020.  
443 ISSN: 1476-4687. <https://www.nature.com/articles/nature07950> (2026) (Apr.  
444 2009).
- 445 17. Stone, L. The stability of mutualism. *Nature Communications* **11**, 2648. ISSN: 2041-1723.  
446 <https://pmc.ncbi.nlm.nih.gov/articles/PMC7253468/> (2026) (May 2020).
- 447 18. Wolin, C. L. & Lawlor, L. R. Models of Facultative Mutualism: Density Effects. *The American*  
448 *Naturalist* **124**. Publisher: The University of Chicago Press, 843–862. ISSN: 0003-0147.  
449 <https://www.journals.uchicago.edu/doi/abs/10.1086/284320> (2026) (Dec. 1984).
- 450 19. Okuyama, T. & Holland, J. N. Network structural properties mediate the stability of mutual-  
451 istic communities. en. *Ecology Letters* **11**. \_eprint: [https://onlinelibrary.wiley.com/doi/pdf/10.1111/j.1461-  
452 0248.2007.01137.x](https://onlinelibrary.wiley.com/doi/pdf/10.1111/j.1461-0248.2007.01137.x), 208–216. ISSN: 1461-0248. [https://onlinelibrary.wiley.com/  
453 doi/abs/10.1111/j.1461-0248.2007.01137.x](https://onlinelibrary.wiley.com/doi/abs/10.1111/j.1461-0248.2007.01137.x) (2026) (2008).
- 454 20. Hale, K. R. S. & Valdovinos, F. S. Ecological theory of mutualism: Robust patterns of stabil-  
455 ity and thresholds in two-species population models. en. *Ecology and Evolution* **11**. \_eprint:  
456 <https://onlinelibrary.wiley.com/doi/pdf/10.1002/ece3.8453>, 17651–17671. ISSN: 2045-7758.  
457 <https://onlinelibrary.wiley.com/doi/abs/10.1002/ece3.8453> (2026) (2021).
- 458 21. Holland, J. N., DeAngelis, D. L. & Bronstein, J. L. Population Dynamics and Mutualism: Func-  
459 tional Responses of Benefits and Costs. *The American Naturalist* **159**. Publisher: The Uni-  
460 versity of Chicago Press, 231–244. ISSN: 0003-0147. [https://www.journals.uchicago.  
461 edu/doi/abs/10.1086/338510](https://www.journals.uchicago.edu/doi/abs/10.1086/338510) (2026) (Mar. 2002).
- 462 22. Niehaus, L. *et al.* Microbial coexistence through chemical-mediated interactions. *Nature*  
463 *Communications* **10**. Publisher: Nature Publishing Group, 1–12. ISSN: 2041-1723. <https://www.nature.com/articles/s41467-019-10062-x> (2022) (May 2019).
- 464 23. Hoek, T. A. *et al.* Resource Availability Modulates the Cooperative and Competitive Nature  
465 of a Microbial Cross-Feeding Mutualism. *PLOS Biology* **14**. Publisher: Public Library of  
466 Science, e1002540. ISSN: 1545-7885. [https://journals.plos.org/plosbiology/  
467 article?id=10.1371/journal.pbio.1002540](https://journals.plos.org/plosbiology/article?id=10.1371/journal.pbio.1002540) (2022) (Aug. 2016).
- 468 24. Johnson, C. A. & Bronstein, J. L. Coexistence and competitive exclusion in mutualism. en.  
469 *Ecology* **100**. \_eprint: <https://esajournals.onlinelibrary.wiley.com/doi/pdf/10.1002/ecy.2708>,  
470 e02708. ISSN: 1939-9170. [https://onlinelibrary.wiley.com/doi/abs/10.1002/  
471 ecy.2708](https://onlinelibrary.wiley.com/doi/abs/10.1002/ecy.2708) (2026) (2019).
- 472 25. MacArthur, R. Species packing, and what competition minimizes. *Proceedings of the Na-*  
473 *tional Academy of Sciences* **64**. Publisher: Proceedings of the National Academy of Sci-  
474 ences, 1369–1371. ISSN: 0027-8424. <https://www.pnas.org/content/64/4/1369>  
475 (2021) (Dec. 1969).
- 476 26. O'Dwyer, J. P. Whence Lotka-Volterra?: Conservation laws and integrable systems in ecol-  
477 ogy. *Theoretical Ecology* **11**. Publisher: Springer Netherlands, 441–452. ISSN: 18741746.  
478 <https://link.springer.com/article/10.1007/s12080-018-0377-0> (2022) (Dec.  
479 2018).
- 480 27. Letten, A. D., Ke, P. J. & Fukami, T. Linking modern coexistence theory and contemporary  
481 niche theory. *Ecological Monographs* **87**. Publisher: John Wiley & Sons, Ltd, 161–177. ISSN:  
482 1557-7015. <https://onlinelibrary.wiley.com/doi/full/10.1002/ecm.1242> (2022)  
483 (May 2017).
- 484 28. Chesson, P. Mechanisms of Maintenance of Species Diversity. en. *Annual Review of Ecol-*  
485 *ogy, Evolution, and Systematics* **31**. Publisher: Annual Reviews, 343–366. ISSN: 1543-  
486 592X, 1545-2069. [https://www.annualreviews.org/content/journals/10.1146/  
487 annurev.ecolsys.31.1.343](https://www.annualreviews.org/content/journals/10.1146/annurev.ecolsys.31.1.343) (2024) (Nov. 2000).
- 488

- 489 29. Koffel, T., Daufresne, T. & Klausmeier, C. A. From competition to facilitation and mutualism:  
490 a general theory of the niche. *Ecological Monographs* **91**. Publisher: John Wiley & Sons,  
491 Ltd, e01458. ISSN: 1557-7015. [https://onlinelibrary.wiley.com/doi/full/10.](https://onlinelibrary.wiley.com/doi/full/10.1002/ecm.1458)  
492 [1002/ecm.1458](https://onlinelibrary.wiley.com/doi/full/10.1002/ecm.1458) (2023) (Aug. 2021).
- 493 30. Meszena, G., Gyllenberg, M., Pasztor, L. & Metz, J. A. Competitive exclusion and limiting  
494 similarity: A unified theory. *Theoretical Population Biology* **69**. Publisher: Academic Press,  
495 68–87. ISSN: 0040-5809. (2022) (Feb. 2006).
- 496 31. Momeni, B., Xie, L. & Shou, W. Lotka-Volterra pairwise modeling fails to capture diverse  
497 pairwise microbial interactions. *eLife* **6**. Publisher: eLife Sciences Publications Ltd. ISSN:  
498 2050084X. (2022) (Mar. 2017).
- 499 32. Letten, A. D. & Stouffer, D. B. The mechanistic basis for higher-order interactions and non-  
500 additivity in competitive communities. *Ecology Letters* **22**. Publisher: John Wiley & Sons,  
501 Ltd, 423–436. ISSN: 1461-0248. [https://onlinelibrary.wiley.com/doi/full/10.](https://onlinelibrary.wiley.com/doi/full/10.1111/ele.13211)  
502 [1111/ele.13211](https://onlinelibrary.wiley.com/doi/full/10.1111/ele.13211) (2023) (Mar. 2019).
- 503 33. Vet, S. *et al.* Bistability in a system of two species interacting through mutualism as well as  
504 competition: Chemostat vs. Lotka-Volterra equations. en. *PLOS ONE* **13**. Publisher: Public  
505 Library of Science, e0197462. ISSN: 1932-6203. [https://journals.plos.org/plosone/](https://journals.plos.org/plosone/article?id=10.1371/journal.pone.0197462)  
506 [article?id=10.1371/journal.pone.0197462](https://journals.plos.org/plosone/article?id=10.1371/journal.pone.0197462) (2026) (June 2018).
- 507 34. Novak, M. *et al.* Characterizing Species Interactions to Understand Press Perturbations:  
508 What Is the Community Matrix? *Annual Review of Ecology, Evolution, and Systematics* **47**.  
509 Publisher: Annual Reviews Inc., 409–432. ISSN: 15452069. (2022) (Nov. 2016).
- 510 35. Tilman, D. Resources: A Graphical-Mechanistic Approach to Competition and Predation.  
511 Source: *The American Naturalist* **116**, 362–393. <https://about.jstor.org/terms> (2022)  
512 (1980).
- 513 36. Meacock, O. J. & Mitri, S. Environment-Organism Feedbacks Drive Changes in Ecological  
514 Interactions. en. *Ecology Letters* **28**. eprint: <https://onlinelibrary.wiley.com/doi/pdf/10.1111/ele.70027>,  
515 e70027. ISSN: 1461-0248. [https://onlinelibrary.wiley.com/doi/abs/10.1111/](https://onlinelibrary.wiley.com/doi/abs/10.1111/ele.70027)  
516 [ele.70027](https://onlinelibrary.wiley.com/doi/abs/10.1111/ele.70027) (2025) (2025).
- 517 37. Cui, W., Marsland, R. & Mehta, P. Les Houches Lectures on Community Ecology: From Niche  
518 Theory to Statistical Mechanics. *ArXiv*, arXiv:2403.05497v1. ISSN: 2331-8422. [https://](https://www.ncbi.nlm.nih.gov/pmc/articles/PMC10942479/)  
519 [www.ncbi.nlm.nih.gov/pmc/articles/PMC10942479/](https://www.ncbi.nlm.nih.gov/pmc/articles/PMC10942479/) (2024) (Mar. 2024).
- 520 38. Picot, A., Shibasaki, S., Meacock, O. J. & Mitri, S. Microbial interactions in theory and  
521 practice: when are measurements compatible with models? en. *Current Opinion in Mi-*  
522 *crobiology* **75**, 102354. ISSN: 1369-5274. [https://www.sciencedirect.com/science/](https://www.sciencedirect.com/science/article/pii/S1369527423000917)  
523 [article/pii/S1369527423000917](https://www.sciencedirect.com/science/article/pii/S1369527423000917) (2023) (Oct. 2023).
- 524 39. Johnson, C. A. How mutualisms influence the coexistence of competing species. en. *Ecol-*  
525 *ogy* **102**. eprint: <https://esajournals.onlinelibrary.wiley.com/doi/pdf/10.1002/ecy.3346>,  
526 e03346. ISSN: 1939-9170. <https://onlinelibrary.wiley.com/doi/abs/10.1002/ecy.3346>  
527 (2026) (2021).
- 528 40. Clark, J. P. The Second Derivative and Population Modeling. en. *Ecology* **52**. eprint: <https://esajournals.onlinelibrary.wiley.com/doi/pdf/10.1002/1934148>,  
529 e0606-613. ISSN: 1939-9170. [https://onlinelibrary.wiley.com/doi/abs/10.2307/](https://onlinelibrary.wiley.com/doi/abs/10.2307/1934148)  
530 [1934148](https://onlinelibrary.wiley.com/doi/abs/10.2307/1934148) (2025) (1971).
- 531 41. Ginzburg, L. R. The theory of population dynamics: I. Back to first principles. *Journal of*  
532 *Theoretical Biology* **122**, 385–399. ISSN: 0022-5193. [https://www.sciencedirect.](https://www.sciencedirect.com/science/article/pii/S0022519386801801)  
533 [com/science/article/pii/S0022519386801801](https://www.sciencedirect.com/science/article/pii/S0022519386801801) (2025) (Oct. 1986).
- 534 42. Shou, W., Ram, S. & Vilar, J. M. G. Synthetic cooperation in engineered yeast populations.  
535 *Proceedings of the National Academy of Sciences* **104**. Publisher: Proceedings of the  
536 National Academy of Sciences, 1877–1882. [https://www.pnas.org/doi/abs/10.1073/](https://www.pnas.org/doi/abs/10.1073/pnas.0610575104)  
537 [pnas.0610575104](https://www.pnas.org/doi/abs/10.1073/pnas.0610575104) (2026) (Feb. 2007).
- 538 43. Dal Co, A., van Vliet, S., Kiviet, D. J., Schlegel, S. & Ackermann, M. Short-range interactions  
539 govern the dynamics and functions of microbial communities. *Nature Ecology and Evolu-*

540  
541  
542  
543  
544  
545  
546  
547  
548  
549  
550  
551  
552  
553  
554  
555  
556  
557  
558  
559  
560  
561  
562  
563  
564  
565  
566  
567  
568  
569  
570  
571  
572  
573  
574  
575  
576  
577  
578  
579  
580  
581  
582  
583  
584  
585  
586  
587  
588  
589  
590

tion **4**. Publisher: Nature Publishing Group, 366–375. ISSN: 2397-334X. <https://www.nature.com/articles/s41559-019-1080-2> (2021) (Feb. 2020).

44. Müller, M. J. I., Neugeboren, B. I., Nelson, D. R. & Murray, A. W. Genetic drift opposes mutualism during spatial population expansion. *Proceedings of the National Academy of Sciences of the United States of America* **111**. Publisher: National Academy of Sciences ISBN: 0027-8424, 1037-1042. ISSN: 0027-8424. <http://www.ncbi.nlm.nih.gov/pubmed/11087846> (2018) (Jan. 2014).

45. Hammarlund, S. P., Chacón, J. M. & Harcombe, W. R. A shared limiting resource leads to competitive exclusion in a cross-feeding system. en. *Environmental Microbiology* **21**. \_eprint: <https://enviromicro-journals.onlinelibrary.wiley.com/doi/pdf/10.1111/1462-2920.14493>, 759–771. ISSN: 1462-2920. <https://onlinelibrary.wiley.com/doi/abs/10.1111/1462-2920.14493> (2025) (2019).

46. Pignon, E., Holló, G., Steiner, T., van Vliet, S. & Schaerli, Y. Uptake and leakage rates differentially shape community arrangement and composition of microbial consortia. *The ISME Journal* **19**, wraf122. ISSN: 1751-7362. <https://doi.org/10.1093/ismejo/wraf122> (2026) (Jan. 2025).

47. Ross, T. D., Im, H., Keogh, B. G., Klausmeier, C. A. & Venturelli, O. S. Metabolic interplay drives population cycles in a cross-feeding microbial community. en. *Nature Communications* **16**. Publisher: Nature Publishing Group, 8919. ISSN: 2041-1723. <https://www.nature.com/articles/s41467-025-63986-y> (2026) (Oct. 2025).

48. McDonald, J. A. K. et al. Evaluation of microbial community reproducibility, stability and composition in a human distal gut chemostat model. *Journal of Microbiological Methods* **95**, 167–174. ISSN: 0167-7012. <https://www.sciencedirect.com/science/article/pii/S0167701213002716> (2026) (Nov. 2013).

49. Hernandez, M. J. Dynamics of transitions between population interactions: A nonlinear interaction  $\chi$ -function defined. *Proceedings of the Royal Society B: Biological Sciences* **265**. Publisher: Royal Society, 1433–1440. ISSN: 14712970. <https://royalsocietypublishing.org/> (2023) (Aug. 1998).

50. Preussger, D., Giri, S., Muhsal, L. K., Oña, L. & Kost, C. Reciprocal Fitness Feedbacks Promote the Evolution of Mutualistic Cooperation. English. *Current Biology* **30**. Publisher: Elsevier, 3580–3590.e7. ISSN: 0960-9822. [https://www.cell.com/current-biology/abstract/S0960-9822\(20\)30986-6](https://www.cell.com/current-biology/abstract/S0960-9822(20)30986-6) (2026) (Sept. 2020).

51. Mee, M. T., Collins, J. J., Church, G. M. & Wang, H. H. Syntrophic exchange in synthetic microbial communities. *Proceedings of the National Academy of Sciences* **111**. Publisher: Proceedings of the National Academy of Sciences, E2149–E2156. <https://www.pnas.org/doi/abs/10.1073/pnas.1405641111> (2025) (May 2014).

52. Chesson, P. MacArthur’s consumer-resource model. *Theoretical Population Biology* **37**, 26–38. ISSN: 0040-5809. <https://www.sciencedirect.com/science/article/pii/S00405809900025Q> (2025) (Feb. 1990).

53. Saavedra, S. et al. A structural approach for understanding multispecies coexistence. en. *Ecological Monographs* **87**. \_eprint: <https://esajournals.onlinelibrary.wiley.com/doi/pdf/10.1002/ecm.1263>, 470–486. ISSN: 1557-7015. <https://onlinelibrary.wiley.com/doi/abs/10.1002/ecm.1263> (2025) (2017).

54. Spaak, J. W. & De Laender, F. Intuitive and broadly applicable definitions of niche and fitness differences. en. *Ecology Letters* **23**. \_eprint: <https://onlinelibrary.wiley.com/doi/pdf/10.1111/ele.13511>, 1117–1128. ISSN: 1461-0248. <https://onlinelibrary.wiley.com/doi/abs/10.1111/ele.13511> (2025) (2020).

55. Song, C., Barabás, G. & Saavedra, S. On the Consequences of the Interdependence of Stabilizing and Equalizing Mechanisms. *The American Naturalist* **194**. Publisher: The University of Chicago Press, 627–639. ISSN: 0003-0147. <https://www.journals.uchicago.edu/doi/full/10.1086/705347> (2024) (Nov. 2019).

- 591 56. May, R. M. Will a Large Complex System be Stable? en. *Nature* **238**. Number: 5364 Pub-  
592 lisher: Nature Publishing Group, 413–414. ISSN: 1476-4687. [https://www.nature.com/  
593 articles/238413a0](https://www.nature.com/articles/238413a0) (2023) (Aug. 1972).
- 594 57. Godoy, O. et al. Cooperation maximizes biodiversity. en. *The American Naturalist*. [https:  
595 //www.journals.uchicago.edu/doi/10.1086/741536](https://www.journals.uchicago.edu/doi/10.1086/741536) (2026) (2026).
- 596 58. Drew, G. C., Stevens, E. J. & King, K. C. Microbial evolution and transitions along the  
597 parasite–mutualist continuum. en. *Nature Reviews Microbiology* **19**. Number: 10 Publisher:  
598 Nature Publishing Group, 623–638. ISSN: 1740-1534. [https://www.nature.com/articles/  
599 s41579-021-00550-7](https://www.nature.com/articles/s41579-021-00550-7) (2024) (Oct. 2021).
- 600 59. Palmer, J. D. & Foster, K. R. Bacterial species rarely work together. *Science* **376**. Publisher:  
601 American Association for the Advancement of Science, 581–582. ISSN: 10959203. [https:  
602 //www.science.org/doi/10.1126/science.abn5093](https://www.science.org/doi/10.1126/science.abn5093) (2023) (May 2022).
- 603 60. Hammarlund, S. P., Gedeon, T., Carlson, R. P. & Harcombe, W. R. Limitation by a shared mu-  
604 tualist promotes coexistence of multiple competing partners. en. *Nature Communications*  
605 **12**. Publisher: Nature Publishing Group, 619. ISSN: 2041-1723. [https://www.nature.  
606 com/articles/s41467-021-20922-0](https://www.nature.com/articles/s41467-021-20922-0) (2026) (Jan. 2021).
- 607 61. Thompson, J. N. Variation in Interspecific Interactions. *Annual Review of Ecology and Sys-  
608 tematics* **19**. Publisher: Annual Reviews, 65–87. ISSN: 0066-4162. [https://www.jstor.  
609 org/stable/2097148](https://www.jstor.org/stable/2097148) (2026) (1988).
- 610 62. Orr, J. A., Armitage, D. W. & Letten, A. D. Coexistence Theory for Microbial Ecology, and  
611 Vice Versa. en. *Environmental Microbiology* **27**. Publisher: John Wiley & Sons, Ltd, e70072.  
612 ISSN: 1462-2920. [https://enviromicro-journals.onlinelibrary.wiley.com/doi/  
613 10.1111/1462-2920.70072](https://enviromicro-journals.onlinelibrary.wiley.com/doi/10.1111/1462-2920.70072) (2026) (Mar. 2025).
- 614 63. Sakarchi, J. & Germain, R. M. MacArthur’s Consumer–Resource Model: A Rosetta Stone  
615 for Competitive Interactions. *The American Naturalist* **205**. Publisher: The University of  
616 Chicago Press, 306–326. ISSN: 0003-0147. [https://www.journals.uchicago.edu/  
617 doi/full/10.1086/733516](https://www.journals.uchicago.edu/doi/full/10.1086/733516) (2025) (Mar. 2025).
- 618 64. Pastore, A. I., Barabás, G., Bimler, M. D., Mayfield, M. M. & Miller, T. E. The evolution of niche  
619 overlap and competitive differences. en. *Nature Ecology & Evolution* **5**. Publisher: Nature  
620 Publishing Group, 330–337. ISSN: 2397-334X. [https://www.nature.com/articles/  
621 s41559-020-01383-y](https://www.nature.com/articles/s41559-020-01383-y) (2026) (Mar. 2021).
- 622 65. Chesson, P. & Kuang, J. J. The interaction between predation and competition. en. *Nature*  
623 **456**. Publisher: Nature Publishing Group, 235–238. ISSN: 1476-4687. [https://www.  
624 nature.com/articles/nature07248](https://www.nature.com/articles/nature07248) (2025) (Nov. 2008).
- 625 66. Colyvan, M. & Ginzburg, L. R. The Galilean turn in population ecology. en. *Biology and Phi-  
626 losophy* **18**, 401–414. ISSN: 1572-8404. [https://doi.org/10.1023/A:1024121002194  
627 \(2025\) \(June 2003\).](https://doi.org/10.1023/A:1024121002194)
- 628 67. Ciarmoli, B. & Marbach, S. *Recycling and complementary food sources hinder oscillatory  
629 dynamics in a microbial population* en. ISSN: 2692-8205 Pages: 2025.09.22.677798 Sec-  
630 tion: New Results. Sept. 2025. [https://www.biorxiv.org/content/10.1101/2025.09.  
631 22.677798v1](https://www.biorxiv.org/content/10.1101/2025.09.22.677798v1) (2026).
- 632 68. Yang, Y., Foster, K. R., Coyte, K. Z. & Li, A. Time delays modulate the stability of complex  
633 ecosystems. en. *Nature Ecology & Evolution* **7**. Publisher: Nature Publishing Group, 1610–  
634 1619. ISSN: 2397-334X. [https://www.nature.com/articles/s41559-023-02158-x  
635 \(2025\) \(Oct. 2023\).](https://www.nature.com/articles/s41559-023-02158-x)
- 636 69. Van den Berg, N. I. et al. Ecological modelling approaches for predicting emergent proper-  
637 ties in microbial communities. en. *Nature Ecology & Evolution* **6**. Publisher: Nature Publish-  
638 ing Group, 855–865. ISSN: 2397-334X. [https://www.nature.com/articles/s41559-  
639 022-01746-7](https://www.nature.com/articles/s41559-022-01746-7) (2025) (July 2022).
- 640 70. Liu, X., Constable, G. W. A. & Pitchford, J. W. Feasibility and stability in large Lotka Volterra  
641 systems with interaction structure. *Physical Review E* **107**. Publisher: American Physical

642  
643

Society, 054301. <https://link.aps.org/doi/10.1103/PhysRevE.107.054301> (2025)  
(May 2023).

# Emergent competition resolves the paradox of stable microbial mutualisms – Supplementary Information

Oliver J. Meacock  \*<sup>1</sup> and Sara Mitri  <sup>2</sup>

<sup>1</sup>School of Biosciences, University of Sheffield, Sheffield, United Kingdom

<sup>2</sup>Department of Fundamental Microbiology, University of Lausanne, Lausanne, Switzerland

## 1 Supplementary methods

### 1.1 Auxotrophy model

#### 1.1.1 Formulation

Species in the auxotrophy model depend on both an in-common carbon source that all members of the community rely on (e.g. glucose) and a species-specific amino acid that they alone rely on [1]. The co-essentiality of these two resources is represented by using the product of separate Monod functions for the two resources when determining growth rates and resource utilisation rates. We additionally include a metabolic shunt that enables production of cross-fed amino acids even when the essential amino acid for a given species is not available [2]. This ensures that amino acid secretion is not directly coupled to growth, allowing the community to begin secreting amino acids into the input media even when it contains only the raw carbon source. The community can thus establish in amino-acid free media (Fig. S1). The rate of amino acid secretion is determined purely by the carbon source availability, again transformed via a Monod function.

We arrange the environment vector  $r$  so that amino acid in position  $\rho$  corresponds to the amino acid required by the species with the same index (i.e. so that  $\rho = \alpha$  for auxotroph  $\alpha$  and required amino acid  $\rho$ ). The in-common carbon source is placed in the final position of the vector with index  $N + 1$  (where  $N$  is the number of auxotrophic populations). The sensitivity function is then defined as:

$$g_{\alpha} = \nu_{\alpha} \frac{r_{\alpha}}{r_{\alpha} + K_{\alpha\alpha}} \frac{r_{N+1}}{r_{N+1} + K_{\alpha(N+1)}} - D, \quad (\text{S.1})$$

where  $D$  is the dilution rate of the chemostat,  $K_{\alpha(N+1)}$  and  $K_{\alpha\alpha}$  are the half-velocity constants for the carbon source and consumed amino acid respectively and  $\nu_{\alpha}$  is the maximal growth rate.

The impact function is additionally defined as:

---

\*o.meacock@sheffield.ac.uk

$$f_{\alpha\rho} = \begin{cases} -\frac{1}{Y_{\alpha\rho}}\nu_{\alpha}\frac{r_{\rho}}{r_{\rho}+K_{\alpha\rho}}\frac{r_{(N+1)}}{r_{(N+1)}+K_{\alpha(N+1)}} & \text{if } \rho = \alpha \text{ (}\rho \text{ is missing amino acid)} \\ -\frac{1}{Y_{\alpha\rho}}\nu_{\alpha}\frac{r_{\alpha}}{r_{\alpha}+K_{\alpha\alpha}}\frac{r_{\rho}}{r_{\rho}+K_{\alpha\rho}} - \nu_{\alpha}\frac{r_{\rho}}{r_{\rho}+K_{\alpha\rho}} \sum_{\gamma \neq \{\alpha, N+1\}} \ell_{\alpha\gamma} & \text{if } \rho = N+1 \text{ (}\rho \text{ is carbon source)} \\ \nu_{\alpha}\ell_{\alpha\rho}\frac{r_{(N+1)}}{r_{(N+1)}+K_{\alpha(N+1)}} & \text{otherwise (}\rho \text{ is secreted amino acid)} \end{cases} \quad (\text{S.2})$$

29 where we have introduced the scaled production rate of amino acid  $\rho$  by species  $\alpha$  as  $\ell_{\alpha\rho}$  and  
 30 the yield of species  $\alpha$  on amino acid/carbon source  $\rho$  as  $Y_{\alpha\rho}$ .

31 Finally, we define the allogenic function using the standard form for chemostat-type systems,  
 32  $\sigma = D(r_{\text{IN}} - r)$ , where  $r_{\text{IN}}$  is the composition of the input media.

### 33 1.1.2 Simulations

34 We provide parameter values for the 2-species model in table S2. In some cases, we suppress  
 35 the species label where this is clear from context to simplify notation (for example,  $\hat{v}$  is the only  
 36 species that secretes  $w$ , so we write  $\ell_w$  rather than  $\ell_{\hat{v}w}$ ). Note that some parameters ( $\ell_v$ ,  $\ell_w$ ,  
 37  $D$ ,  $[v]_{\text{IN}}$  and  $[w]_{\text{IN}}$ ) are modified during some analyses, in which case they are specified on plot  
 38 axes, in the relevant figure's caption, or were drawn randomly (see next section).

39 SciPy's `solve_ivp` function was used to numerically integrate the resulting systems of coupled  
 40 ODEs using the Runge-Kutta method of order 5(4).

### 41 1.1.3 Random sampling

42 Parameters for the randomly sampled mechanistic sweep (Figs. 5, S7) were selected from uni-  
 43 form distributions. The amino acid production rates  $\ell_v$  and  $\ell_w$  were drawn from the range  $[0, 1.5]$ ,  
 44 while the input concentrations  $v_{\text{IN}}$  and  $w_{\text{IN}}$  were drawn from the range  $[0, 1]$ . The dynamics of the  
 45 resulting model was numerically integrated until reaching an equilibrium state. The resulting  
 46 system was then mapped onto niche overlap and fitness difference axes (Supplementary Note  
 47 2.3.3) and placed into a  $15 \times 15$  grid covering the niche overlaps between 0 and 1 and the fitness  
 48 differences between 0.1 and 10. Mechanistic parameters (Fig. 5 and effective gLV parameters  
 49 (Fig. S7) were binned according to the position of the final system in this grid. Systems that fell  
 50 outside this region (including systems with positive values of  $a'_{\alpha\beta}$ , see main text) were excluded  
 51 from further analysis. This procedure was repeated 100,000 times, building up a collection of  
 52 underlying parameters for each bin. The collection in each bin was then averaged to give the  
 53 final heatmaps.

54 For the randomly parameterised 5-species model presented in Fig. S6, we drew the values of  
 55  $K_{\alpha\rho}$ ,  $Y_{\alpha\rho}$ ,  $\nu_{\alpha}$  and  $\ell_{\alpha\rho}$  from random distributions.  $K_{\alpha\rho}$ s were drawn uniformly from the range  
 56  $[0.75, 1.25]$ .  $Y_{\alpha\alpha}$ s (the yield of the amino acids) were drawn uniformly from the range  $[15, 25]$ ,  
 57 while  $Y_{\alpha, (N+1)}$  (the yield of the carbon source) was set at 1.  $\nu_{\alpha}$ s were drawn from  $[9, 11]$ .  $\phi_{\alpha\rho}$ s  
 58 was constructed by drawing values uniformly from the range  $[-0.1, 0.4]$  and clipping the nega-  
 59 tive part of the resulting distribution to zero, simulating amino acids that are not produced by  
 60  $\alpha$ . We additionally set  $\phi_{\alpha\alpha} = 0$  to prevent secretion of the amino acid  $\alpha$  was auxotrophic for  
 61 and  $\phi_{\alpha(N+1)} = 0$  to prevent secretion of the carbon source. The resulting set of random values  
 62 was scaled by a constant that allowed us to vary the average production rate, which was swept  
 63 systematically from 0.001 to 0.3. The 'average production rate' is the average of all production  
 64 rates following this scaling. We fed the simulated community in the chemostat on media con-  
 65 taining the carbon source at concentration  $r_{(N+1)} = 1$  and no amino acids. All populations were  
 66 inoculated at density 0.05. The dilution rate  $D$  was 0.05.

## 2 Supplementary Notes

### 2.1 Supplementary Note 1: Derivation of EO equations

To derive the accelerational EO (aEO) equation (Eq. 5), we find the temporal derivative of the PCGR of a focal species  $\alpha$  in an EO system. Starting with our definition of the sensitivity function  $g_\alpha(\mathbf{r})$  as the PCGR at  $\mathbf{r}$  (Eq. 3), we obtain

$$\frac{d}{dt} \left( \frac{1}{x_\alpha} \frac{dx_\alpha}{dt} \right) = \frac{dg_\alpha(\mathbf{r})}{dt} \quad (\text{S.3})$$

Applying the chain rule yields

$$\frac{d}{dt} \left( \frac{1}{x_\alpha} \frac{dx_\alpha}{dt} \right) = \nabla g_\alpha \cdot \frac{d\mathbf{r}}{dt}. \quad (\text{S.4})$$

Next, we substitute the definition of the rate of environmental change (Eq. 2)

$$\frac{d}{dt} \left( \frac{1}{x_\alpha} \frac{dx_\alpha}{dt} \right) = \nabla g_\alpha \cdot \boldsymbol{\sigma} + \sum_{\beta} \nabla g_\alpha \cdot \mathbf{f}_\beta x_\beta. \quad (\text{S.5})$$

Applying the definitions of the abiotic acceleration  $\mu'_\alpha(\mathbf{r}) \equiv \boldsymbol{\sigma}(\mathbf{r}) \cdot \nabla g_\alpha(\mathbf{r})$  and the biotic acceleration  $a'_{\alpha\beta}(\mathbf{r}) \equiv \nabla g_\alpha \cdot \mathbf{f}_\beta$  yields the aEO equation:

$$\frac{d}{dt} \left( \frac{1}{x_\alpha} \frac{dx_\alpha}{dt} \right) = \mu'_\alpha(\mathbf{r}) + \sum_{\beta} a'_{\alpha\beta}(\mathbf{r}) x_\beta. \quad (\text{S.6})$$

As noted in the main text, in an equilibrium environment  $\frac{d}{dt} \left( \frac{1}{x_\alpha} \frac{dx_\alpha}{dt} \right) = 0$ . Applying this assumption to the aEO equation results in the equilibrium Environment Organism (eEO) equation:

$$0 = \mu'_\alpha(\mathbf{r}^*) + \sum_{\beta} a'_{\alpha\beta}(\mathbf{r}^*) x_\beta, \quad (\text{S.7})$$

In previous work [3], we derived two expressions which describe PCGRs in EO-type ecosystems under regimes in which the environment can change: the closed Environment-Organism (cEO) and fluctuating Environment-Organism (fEO) equations. While we previously derived these using a path integral approach, they can also be derived directly from the aEO equation. Integrating Eq. 5 yields the fEO equation

$$\frac{1}{x_\alpha} \frac{dx_\alpha}{dt} = g_\alpha(\mathbf{r}_0) + \int_0^t \mu'_\alpha(\mathbf{r}) \cdot d\tau + \sum_{\beta} \int_0^t a'_{\alpha\beta}(\mathbf{r}) x_\beta \cdot d\tau. \quad (\text{S.8})$$

This describes the current growth rate of  $\alpha$  based on the history of its interactions with other species and allogenic processes, along with an initial growth rate  $g_\alpha(\mathbf{r}_0)$ . In closed systems  $\mu'_\alpha = 0$ , yielding the cEO equation:

$$\frac{1}{x_\alpha} \frac{dx_\alpha}{dt} = g_\alpha(\mathbf{r}_0) + \sum_{\beta} \int_0^t a'_{\alpha\beta}(\mathbf{r}) x_\beta \cdot d\tau. \quad (\text{S.9})$$

86 This family of equations represents different experimental scenarios. The cEO equation de-  
87 scribes the dynamics of closed well-mixed systems (e.g. batch culture) and spatially structured  
88 systems under one dimensional flow (e.g. the lower gut) [3]. The fEO and aEO equations in  
89 turn describe open systems undergoing changes in environmental composition over time (e.g.  
90 seasonal variations in a lake), while the eEO equation captures open systems at equilibrium  
91 (e.g. a stable bioreactor). When a community with a given set of impacts and sensitivities is  
92 placed in these different contexts, we observe distinct but related dynamical outcomes. These  
93 equations allow us to formally relate these different outcomes to each other.

## 2.2 Supplementary Note 2: Comparison of separation of timescales and the accelerational mapping

Obtaining a general mapping between mechanistic theories and direct interaction models has been a long sought-after goal of theoretical ecology, as it would allow us to cast the interaction structure of ecosystems in terms of underlying biological mechanisms [4]. The standard way of approaching the problem is to assume a separation in the timescales of the environmental and population dynamics [5], as first introduced by MacArthur [6]. In brief, environmental variables are forced to equilibrate by setting Eq. 2 to zero, resulting in an algebraic constraint which can be substituted into Eq. 3. The construction of MacArthur’s model ensures that the resulting composite coefficients can be mapped onto those of the gLV equation as constants.

While influential, this approach to the problem is brittle. Firstly, there is generally no natural separation between the two timescales, with environmental dynamics occurring at approximately the same rate as the population dynamics. Even more problematically for the study of systems fueled by abiotic resources, the mapping is not possible unless the environmental variables themselves have logistic dynamics (*i.e.* act as biotic resources with density-dependent reproduction rates) [4]. Separation of timescales is additionally used in other theoretical studies that do not assume logistic resource dynamics (*e.g.* [7]). However, the resulting models cannot be framed in terms of the gLV equation.

Our accelerational approach avoids these issues, providing a general and flexible mapping between the two frameworks. We can illustrate the differences between the two approaches by comparing the output of the EO mapping to MacArthur’s original results. MacArthur’s consumer-resource model can be written as:

$$\frac{1}{x_\alpha} \frac{dx_\alpha}{dt} = \left( \sum_\rho w_\rho p_{\rho\alpha} r_\rho \right) - m_\alpha, \quad (\text{S.10a})$$

$$\frac{dr_\rho}{dt} = \frac{r_\rho \nu_\rho}{k_\rho} (k_\rho - r_\rho) - r_\rho \sum_\beta p_{\rho\beta} x_\beta, \quad (\text{S.10b})$$

where  $k_\rho$  is the carrying capacity for biotic resource  $\rho$ ,  $p_{\rho\alpha}$  represents the rate at which  $\rho$  is consumed by species  $\alpha$  and converted to its own biomass,  $w_\rho$  is the nutritional value of  $\rho$ ,  $\nu_\rho$  is the maximal rate of increase of  $\rho$  and  $m_\alpha$  is  $\alpha$ ’s mortality rate (note that terms representing biomass conversion efficiency have been set to unity to simplify the expressions while retaining the structure of the model).

Separation of timescales yields the phenomenological gLV parameters [6]

$$a_{\alpha\beta} = - \sum_\rho p_{\rho\alpha} p_{\rho\beta} w_\rho \frac{k_\rho}{\nu_\rho}, \quad (\text{S.11a})$$

$$\mu_\alpha = \sum_\rho k_\rho w_\rho p_{\rho\alpha} - m_\alpha. \quad (\text{S.11b})$$

To apply our timescale separation-free approach, we begin by writing equation S.11b in terms of impact, sensitivity and allogenic functions (Table S1). Application of the definitions of  $\mu'_\alpha$  and  $a'_{\alpha\beta}$  yields

$$a'_{\alpha\beta} = - \sum_{\rho} p_{\rho\alpha} p_{\rho\beta} w_{\rho} r_{\rho}^*, \quad (\text{S.12a})$$

$$\mu'_{\alpha} = \sum_{\rho} \frac{r_{\rho}^* \nu_{\rho}}{k_{\rho}} (k_{\rho} - r_{\rho}^*) w_{\rho} p_{\rho\alpha}. \quad (\text{S.12b})$$

125 As the PCGA-based parameterisation depends on the equilibrium environment  $\mathbf{r}^*$ , we must  
 126 also identify this composition. In this case, this is given by the intersection of Zero Net Growth  
 127 Isoclines (ZNGIs) where  $g_{\alpha} = 0$  for all species [8, 9]. Assuming the number of resources is  
 128 equal to the number of species, this occurs at  $\mathbf{r}^* = \mathbf{m}M^{-1}$ , where the elements of the matrix  
 129  $M$  are  $M_{\rho\alpha} = w_{\rho} p_{\rho\alpha}$  and  $\mathbf{m}$  is the vector of mortalities  $m_{\alpha}$ .

130 Comparing the two results, we note that the units of  $a_{\alpha\beta}$  and  $\mu_{\alpha}$  are  $[\text{Time}]^{-1}[\text{Biomass}]^{-1}$  and  
 131  $[\text{Time}]^{-1}$  respectively, while those of  $a'_{\alpha\beta}$  and  $\mu'_{\alpha}$  are  $[\text{Time}]^{-2}[\text{Biomass}]^{-1}$  and  $[\text{Time}]^{-2}$ . The  
 132 additional unit of inverse time in the accelerational quantities corresponds to the timescale of  
 133 the resource dynamics, which is no longer eliminated through separation of timescales.

134 We also observe that the definitions of both  $a_{\alpha\beta}$  and  $a'_{\alpha\beta}$  consist of the sum of the products of  
 135 the consumption rates  $p_{\rho\alpha} p_{\rho\beta}$  with a factor that only depends on the resource index ( $w_{\rho} \frac{k_{\rho}}{\nu_{\rho}}$  for  
 136  $a_{\alpha\beta}$  and  $w_{\rho} r_{\rho}^*$  for  $a'_{\alpha\beta}$ ). In Chesson's analysis of MacArthur's model [10], the  $w_{\rho} \frac{k_{\rho}}{\nu_{\rho}}$ s become the  
 137 weights in a weighted least-squares regression between  $p_{\rho\alpha}$  and  $p_{\rho\beta}$ , with the square root of  
 138 the resulting coefficient of determination  $R^2$  then being proportional to the niche overlap (see  
 139 also Supplementary Note 2.3.3). The similarities in the structure of the expressions for  $a_{\alpha\beta}$  and  
 140  $a'_{\alpha\beta}$  means that this argument also applies to the acceleration-based analysis of MacArthur's  
 141 model, allowing us to relate niche overlap to the linear independence of the utilisation vectors  
 142  $\mathbf{p}_{\alpha}$  and  $\mathbf{p}_{\beta}$ .

## 2.3 Supplementary Note 3: Equivalencies between rate-based and accelerational ecological frameworks

In the main text, we note that the eEO equation (Eq. S.7) is structurally equivalent to the gLV equation at equilibrium. In this Note, we discuss several concepts that can be translated between the two frameworks on the basis of this equivalence: carrying capacity, linear stability and the stabilising/equalising mechanisms of Modern Coexistence Theory (MCT).

### 2.3.1 Carrying capacity

In Lotka-Volterra type systems, the carrying capacity of a species  $K_\alpha$  is defined as its equilibrium abundance in isolation:

$$\frac{1}{x_\alpha} \frac{dx_\alpha}{dt} = \mu_\alpha + a_{\alpha\alpha} x_\alpha \quad (\text{S.13a})$$

$$\implies 0 = \mu_\alpha + a_{\alpha\alpha} K_\alpha \quad (\text{S.13b})$$

$$\implies K_\alpha = -\frac{\mu_\alpha}{a_{\alpha\alpha}}. \quad (\text{S.13c})$$

This captures the concept of self-limitation in ecosystems – assuming  $a_{\alpha\alpha}$  is negative (due to self-competition) and  $\mu_\alpha$  is positive (i.e.  $\alpha$  can establish in the current environment in isolation),  $K_\alpha$  is a positive, finite value that indicates the density of  $\alpha$  at which competition with itself exactly balances its underlying ability to grow.

Similar logic can be applied to obtain an equivalent expression for our accelerational framework:

$$\frac{d}{dt} \left( \frac{1}{x_\alpha} \frac{dx_\alpha}{dt} \right) = \mu'_\alpha + a'_{\alpha\alpha} x_\alpha \quad (\text{S.14a})$$

$$\implies 0 = \mu'_\alpha + a'_{\alpha\alpha} K_\alpha \quad (\text{S.14b})$$

$$\implies K_\alpha = -\frac{\mu'_\alpha}{a'_{\alpha\alpha}} = -\frac{\nabla g_\alpha \cdot \boldsymbol{\sigma}}{\nabla g_\alpha \cdot \mathbf{f}_\alpha}. \quad (\text{S.14c})$$

Though equivalent in structure, this equation gives us a deeper mechanistic understanding of self-limitation. For example, we can see that increasing the elements of  $\boldsymbol{\sigma}$  representing input of beneficial environmental factors (for which  $\nabla g_{\alpha\rho}$  is positive) and decreasing the input of harmful environmental factors (for which  $\nabla g_{\alpha\rho}$  is negative) will generally increase the value of the numerator, raising the overall value of  $K_\alpha$ . The denominator is a more complex structure, particularly as trade-offs may enforce correlations between the elements of the vectors  $\nabla g_\alpha$  and  $\mathbf{f}_\alpha$ . However, we may broadly expect that an increase in the uptake of beneficial factors and release of harmful factors by  $\alpha$  will make the denominator more negative and so reduce the carrying capacity overall.

An interesting case arises when  $\mu'_\alpha = 0$ , as in closed ecosystems. While this superficially suggests that the carrying capacity is  $K_\alpha = 0$ , in many systems the intra-specific biotic acceleration  $a'_{\alpha\alpha}$  is also equal to 0 at equilibrium. This may arise when the release of growth-promoting substrates is exactly balanced by their uptake, as for example during nutrient cycling by algae [11], or when impacts fall to zero, as at the end of a batch culture experiment once all nutrients have been depleted. Under these conditions the carrying capacity is no longer defined by Eq. S.14,

174 and is instead determined by the initial conditions of the system (e.g. the initial amount of  
 175 available nutrients). This implies that we can obtain very limited information about underlying  
 176 ecological processes from these steady-state abundances in closed systems [12].

### 177 2.3.2 Linear stability analysis

178 Linear stability analysis of dynamical systems proceeds by identifying equilibrium states of  
 179 the system and finding the eigenvalues of the system's Jacobian matrix evaluated at those  
 180 points. Eigenvalues with positive real part indicate that arbitrarily small perturbations from the  
 181 equilibrium state will be amplified by internal dynamics, pushing the system away from that  
 182 point and destabilising the system. For the gLV model, the equilibrium composition  $\mathbf{x}^*$  is given  
 183 by [13]

$$\mathbf{x}^* = -A^{-1}\boldsymbol{\mu}, \quad (\text{S.15})$$

184 and the Jacobian  $J^*$  at this stationary point is given by

$$J^* = \begin{pmatrix} a_{11} x_1^* & a_{12} x_1^* & \dots & a_{1N} x_1^* \\ a_{21} x_2^* & a_{22} x_2^* & \dots & a_{2N} x_2^* \\ \vdots & \vdots & \ddots & \vdots \\ a_{N1} x_N^* & a_{N2} x_N^* & \dots & a_{NN} x_N^* \end{pmatrix} \quad (\text{S.16})$$

$$= \text{diag}(\mathbf{x}^*)A. \quad (\text{S.17})$$

185 Performing equivalent analysis in mechanistic models proceeds by evaluating the Jacobian  
 186 of the entire dynamical system, *i.e.* incorporating both population and environmental dynamics  
 187 (e.g. [14], Appendix A of [15]). By concatenating our expressions for the population and environ-  
 188 mental dynamics and assuming that all populations are at non-zero densities, we obtain

$$J^* = \left( \begin{array}{c|c} \frac{\partial}{\partial x_\beta} \left( \frac{dx_\alpha}{dt} \right) & \frac{\partial}{\partial r_\gamma} \left( \frac{dx_\alpha}{dt} \right) \\ \hline \frac{\partial}{\partial x_\beta} \left( \frac{dr_\rho}{dt} \right) & \frac{\partial}{\partial r_\gamma} \left( \frac{dr_\rho}{dt} \right) \end{array} \right) \text{ at } \mathbf{r}^*, \mathbf{x}^* \quad (\text{S.18})$$

$$= \left( \begin{array}{c|c} 0 & \text{diag}(\mathbf{x}^*)\nabla G \\ \hline F & \frac{\partial}{\partial r_\gamma}(\sigma_\rho + \sum_\beta \mathbf{f}_\beta x_\beta^*) \end{array} \right), \quad (\text{S.19})$$

189 where  $F$  is a matrix consisting of all of the impact functions evaluated at  $\mathbf{r}^*$ ,  $\nabla G$  is the matrix  
 190 of all sensitivity gradients evaluated at  $\mathbf{r}^*$  and  $\rho$  and  $\gamma$  are indices for the environmental factors.  
 191 We show the real part of the eigenvalues of this matrix for the two species and five species  
 192 auxotrophy models in Figs. S4b and S6d, respectively.

193 To understand how this result relates to the gLV-based analysis, let us begin by assuming that  
 194 the environmental dynamics do not depend on the values of the environmental factors within the  
 195 neighbourhood of  $\mathbf{r}^*$  (*i.e.* that  $\frac{\partial}{\partial r_\gamma}(\sigma_\rho + \sum_\beta \mathbf{f}_\beta x_\beta^*) = 0$ ). This results in a  $2 \times 2$  block matrix with  
 196 blocks of zeros on the diagonal, for which the eigenvalues are given by  $\pm\sqrt{\text{eig}(\text{diag}(\mathbf{x}^*)\nabla GF)} =$   
 197  $\pm\sqrt{\text{eig}(\text{diag}(\mathbf{x}^*)A)}$ . In other words, this simplifying assumption yields eigenvalues that are the  
 198 square root of the eigenvalues  $s_k$  that we would obtain from a direct translation of Eq. S.17 from  
 199 rate-based to accelerational quantities.

200 This result implies that combinations of  $A$  and  $\mathbf{x}^*$  that produce at least one positive real eigen-  
 201 value in the gLV framework have corresponding  $A$ 's and  $\mathbf{x}^*$ s in the simplified accelerational  
 202 framework that have at least one positive real eigenvalue. This implies that linear instability  
 203 in the gLV framework corresponds to linear instability in the accelerational framework. Per-  
 204 haps more surprisingly, combinations of  $A$  and  $\mathbf{x}^*$  that produce only negative *real* eigenvalues  
 205 (*i.e.* are stable gLV systems) have corresponding  $A$ 's and  $\mathbf{x}^*$ s which produce paired *imaginary*  
 206 eigenvalues. These correspond to neutrally stable systems, in which perturbations from the  
 207 equilibrium state result in indefinite oscillations around that equilibrium.

208 Clearly the environmental self-regulation represented by  $\frac{\partial}{\partial r_\gamma}(\sigma_\rho + \sum_\beta \mathbf{f}_\beta \mathbf{x}_\beta^*)$  is playing an im-  
 209 portant role in ensuring convergence on the system's fixed point. Let us incorporate these terms  
 210 into our analysis more carefully. Following [16], we can use Schur's formula and note that the  
 211 eigenvalues of a matrix and its transpose are the same to obtain the following defining equation  
 212 for the full system's eigenvalues  $\lambda$ :

$$0 = \det(-\lambda I_N) \det \left( -\lambda I_N - \text{diag}(\mathbf{x}^*) \nabla G \left[ \frac{\partial}{\partial r_\rho}(\sigma_\gamma + \sum_\beta \mathbf{f}_\beta \mathbf{x}_\beta^*) - \lambda I_M \right]^{-1} F \right), \quad (\text{S.20})$$

213 where we denote the identity matrix of size  $N$  as  $I_N$ ,  $N$  is the total number of populations and  
 214  $M$  is the total number of environmental factors. Assuming that the system is not neutrally stable  
 215 ( $\lambda \neq 0$ ), this becomes

$$0 = \det \left( -\lambda I_N - \text{diag}(\mathbf{x}^*) \nabla G \left[ \frac{\partial}{\partial r_\rho}(\sigma_\gamma + \sum_\beta \mathbf{f}_\beta \mathbf{x}_\beta^*) - \lambda I_M \right]^{-1} F \right). \quad (\text{S.21})$$

216 It is difficult to make general statements about this equation. However, it is informative to con-  
 217 sider the case of a chemostat in which only dilution at rate  $D$  contributes to the environmental  
 218 self-regulation (*i.e.*  $\nabla \mathbf{f}_\beta = 0$ ). As  $\frac{\partial \sigma_\gamma}{\partial r_\rho} = -D I_M$  in this case, we obtain

$$0 = \det \left( -\lambda I_N - \text{diag}(\mathbf{x}^*) \nabla G [(-D - \lambda) I_M]^{-1} F \right) \quad (\text{S.22a})$$

$$= \det (\lambda(\lambda + D) I_N - \text{diag}(\mathbf{x}^*) A'). \quad (\text{S.22b})$$

219 Referring to these eigenvalues of  $\text{diag}(\mathbf{x}^*) A'$  as  $s_k$ , we can write the eigenvalues  $\lambda_k$  of the  
 220 dilution-only EO system as

$$\lambda_k(\lambda_k + D) = s_k, \quad (\text{S.23})$$

221 with solution

$$\lambda_k = -\frac{D}{2} \pm \sqrt{\frac{D^2}{4} + s_k}. \quad (\text{S.24})$$

222 The upshot of this analysis is that chemostat-type dilution of the environmental factors tends  
 223 to stabilise the ecosystem. The term outside the square root ( $-\frac{D}{2}$ ) is always real and negative,

224 thus damps down the neutral oscillations that would result if the expression under the square  
 225 root remained negative.

226 From these considerations, we can propose conditions for stability of Eq. S.19: firstly, the accel-  
 227 erational version of Eq. S.17 should have negative real eigenvalues to ensure neutral stability in  
 228 the absence of environmental self-regulation. Secondly, environmental self-regulation should  
 229 be dissipative (e.g. through environmental dilution) to dampen the resulting oscillations. Un-  
 230 fortunately, comparison of the eigenvalue spectra of the accelerational version of Eq. S.17 (Fig.  
 231 S5a) and Eq. S.19 (Fig. S5b) for the two species amino acid production sweep shows this picture  
 232 is overly simplistic. While the eigenvalues of the former are predominantly real and negative,  
 233 we observe complex eigenvalues with negative real part and even positive real eigenvalues at  
 234 the lowest production rates. Given that we observe stability in the full system, the environmen-  
 235 tal self-regulation must be doing more than merely damping neutral oscillations. Nonetheless,  
 236 the similarity in the structure of the two sets of eigenvalues is striking and suggests that the  
 237 eigenvalues of  $\text{diag}(x^*)A'$  may be a good proxy for evaluating system stability under a broad  
 238 range of contexts. Exploring the deeper connections between these two perspectives under a  
 239 wider range of scenarios should be a focus of future work.

### 240 2.3.3 Modern Coexistence Theory

241 Modern Coexistence Theory (MCT) arose as an effort to consolidate coexistence mechanisms  
 242 varying across scales and systems into a limited set of processes operating on similar mathe-  
 243 matical principles [17, 18]. One of its most important conclusions is that influences on species  
 244 coexistence can be mathematically partitioned into equalising mechanisms (processes that re-  
 245 duce the difference in average fitness between species) and stabilising mechanisms (processes  
 246 that reduce the overlap of niches between species) [17]. We will focus on the two-species case  
 247 here, noting in passing that the multi-species case can be investigated through other frame-  
 248 works that may in principle be translated into our accelerational formulation through Eq. 6  
 249 [19].

250 Much of our understanding of MCT comes from two-species gLV systems. For competing  
 251 species labelled 1 and 2, feasibility is determined by the solutions of the equations  $x_1^* =$   
 252  $\frac{a_{22}\mu_1 - a_{12}\mu_2}{a_{11}a_{22} - a_{21}a_{12}}$  and  $x_2^* = \frac{a_{11}\mu_2 - a_{21}\mu_1}{a_{11}a_{22} - a_{21}a_{12}}$ . Combining the feasibility requirements of both species  
 253 implies that

$$\frac{a_{12}}{a_{22}} < \frac{\mu_2}{\mu_1} < \frac{a_{11}}{a_{21}} \quad (\text{S.25})$$

254 must hold for mutual coexistence.

255 One of Chesson's insights was to show that the expression  $\frac{a_{\alpha\beta}}{a_{\alpha\alpha}}$  also appears as the regres-  
 256 sion coefficient between the resource preference vectors in MacArthur's consumer-resource  
 257 model (Supplementary Note 2.2, [10]), allowing this expression describing feasible coexistence  
 258 to be formally related to the degree of similarity between the utilisation of resources by the two  
 259 populations. This led to a form of the feasibility criterion in which each component has been  
 260 multiplied by  $\sqrt{\frac{a_{22}a_{21}}{a_{11}a_{12}}}$ :

$$\sqrt{\frac{a_{12}a_{21}}{a_{11}a_{22}}} < \frac{\mu_1}{\mu_2} \sqrt{\frac{a_{22}a_{21}}{a_{11}a_{12}}} < \sqrt{\frac{a_{11}a_{22}}{a_{12}a_{21}}}. \quad (\text{S.26})$$

261 This expression states that the 'fitnesses ratio'  $\frac{\mu_2}{\mu_1} \sqrt{\frac{a_{22}a_{21}}{a_{11}a_{12}}}$  must be between the 'niche overlap'  
 262  $\sqrt{\frac{a_{12}a_{21}}{a_{11}a_{22}}}$  and its reciprocal for coexistence to be feasible. We must also account for stability,

263 which is guaranteed if  $a_{22}a_{11} > a_{21}a_{12}$ . Thus, stable coexistence results provided both that Eq.  
 264 S.26 holds and the niche overlap term  $\sqrt{\frac{a_{12}a_{21}}{a_{11}a_{22}}}$  is less than 1. This latter condition is essentially  
 265 always met as self-limitation is stronger than partner suppression (*i.e.*  $a_{11}$  is more negative than  
 266  $a_{21}$  and  $a_{22}$  is more negative than  $a_{12}$ ) under competition scenarios.

267 It should be emphasised that Eq. S.26 is not MCT in and of itself, but rather the result of applying  
 268 MCT to the two-species gLV equation as a specific ecosystem model [18]. Alternative definitions  
 269 of niche overlap and fitness differences have been proposed for more general models [19–21],  
 270 although the compatibility of some of these alternative definitions with those of Eq. S.26 has  
 271 been called into question [22].

272 The ability to write MacArthur’s consumer-resource model in gLV form using separation of  
 273 timescales (Section 2.2) has led to its widespread adoption as a basis for interpreting niche  
 274 overlaps and fitness differences in mechanistic terms [9, 10, 22]. Our mapping between mech-  
 275 anistic models and the gLV equation (Eq. 6) allows us to generalise this approach for any mech-  
 276 anistic model by substituting in our effective gLV parameters evaluated at equilibrium:

$$\sqrt{\frac{a'_{12}a'_{21}}{a'_{11}a'_{22}}} < \frac{\mu'_2}{\mu'_1} \sqrt{\frac{a'_{22}a'_{21}}{a'_{11}a'_{12}}} < \sqrt{\frac{a'_{11}a'_{22}}{a'_{12}a'_{21}}}. \quad (\text{S.27})$$

277 We discuss the application of this result to the two species auxotrophy model in the main  
 278 text.

279 One downside of this formulation is that it loses its connection to the mutual invasibility crite-  
 280 rion, which states that both species must be able to invade the other when inoculated at low  
 281 density for them to stably coexist. This is because differing equilibrium environmental states  
 282 may mean that the effective gLV parameters for a resident community with  $N - 1$  species are  
 283 very different to those of the full  $N$  species community. However, the mutual invasibility cri-  
 284 terion is known to have a number of deficiencies as a predictor of coexistence in mechanistic  
 285 models [23]. In the case of our own model, it is impossible for either of the obligate mutualists  
 286 to reach an equilibrium in the absence its partner (Fig. S1), meaning there is no such thing as  
 287 a baseline single-species community which can be subjected to invasion. Our approach may  
 288 provide further insights into the conditions under which the mutual invasibility criterion breaks  
 289 down as a predictor of coexistence.

290 **3 Supplementary Tables**

| Simulated system                        | Sensitivity functions  | Impact functions  | Allogenic function   |
|---|--|---|--|
| Abiotic nutrient competition [7]        | $g_\alpha = \sum_\rho b_\rho c_{\alpha\rho} m_\alpha(r_\rho) - \theta$           | $f_{\alpha\rho} = -c_{\alpha\rho} m_\alpha(r_\rho)$   | $\sigma_\rho = r_\rho \text{IN} - d_\rho r_\rho$               |
| Antibiotic-mediated coexistence [24]    | $g_\alpha = m(r_4) e^{-b_\alpha r_\alpha} - \theta_\alpha$                       | $f_{\alpha\rho} = \begin{cases} c m_\alpha(r_4) & \text{if } \rho = \alpha + 1 \text{ (}\rho \text{ is secreted antibiotic)} \\ -d r_\rho & \text{if } \rho = \alpha + 2 \text{ (}\rho \text{ is degraded antibiotic)} \\ -m_\alpha(r_\rho) & \text{if } \rho = 4 \text{ (}\rho \text{ is nutrient)} \\ 0 & \text{otherwise} \end{cases}$ | $\sigma = D(r_{\text{IN}} - r)$                                |
| Nutrient cross-feeding [25]             | $g_\alpha = \sum_\rho b_{\alpha\rho} c_{\alpha\rho} r_\rho - \theta_\alpha$      | $f_{\alpha\rho} = -c_{\alpha\rho} r_\rho + \sum_\gamma d_{\alpha\rho\gamma} c_{\alpha\gamma} r_\gamma$  | $\sigma = D(r_{\text{IN}} - r)$                                |
| Chemical-mediated interactions [26]     | $g_\alpha = b_\alpha + \sum_\rho (m_\alpha^+(r_\rho) + c_{\alpha\rho}^- r_\rho)$ | $f_{\alpha\rho} = d_{\alpha\rho} - o_{\alpha\rho} m_\alpha(r_\rho)$   | $\sigma = 0$   |
| Tilman's consumer-resource model [8]    | $g_\alpha = m_\alpha(\sum_\rho b_{\alpha\rho} - c_\alpha) - D$                   | $f_{\alpha\rho} = -d_{\alpha\rho}$  | $\sigma = D(r_{\text{IN}} - r)$                                |
| MacArthur's consumer-resource model [6] | $g_\alpha = \sum_\rho b_\rho c_{\alpha\rho} r_\rho - \theta_\alpha$              | $f_{\alpha\rho} = -c_{\alpha\rho} r_\rho$   | $\sigma_\rho = \frac{r_\rho d_\rho}{o_\rho} (o_\rho - r_\rho)$ |

Table S1: **Non-exhaustive list of established EO models.**  $b$ ,  $c$ ,  $d$  and  $o$  are model-specific parameters whose meanings are given below the model specification.  $m_\alpha(r_\rho)$  denotes a Monod function acting on resource  $r_\rho$  with embedded half-velocity and maximal utilization rate constants.  $\theta$  denotes a mortality rate, while  $D$  denotes a dilution rate. Superscripts  $+$  and  $-$  indicate that the associated terms only apply if they are positive or negative, respectively.  $\rho$  and  $\gamma$  are indices of the environment vector  $r$ . Where necessary, the structure of the environment vector with respect to the species index  $\alpha$  is also specified. Note that in some cases, indices in  $r$  are modulo the length of the environment vector (for example, index  $\alpha + 1$  in the antibiotic-mediated coexistence model is written fully as  $(\alpha + 1) \bmod 3$ ). We suppress the modulo operation in these cases for notational compactness. Some additional constraints on parameters present in the original models (e.g. enforcing conservation of mass) are not specified. Please see cited publications for complete model specifications including parameter choices.

| Parameter symbol  | Parameter meaning                                  | Value |
|-------------------|--|-------|
| $\nu_{\hat{v}}$   | Maximum growth rate of $\hat{v}$                   | 0.4   |
| $\nu_{\hat{w}}$   | Maximum growth rate of $\hat{w}$                   | 0.4   |
| $K_{\hat{v} c}$   | Half velocity constant for use of $c$ by $\hat{v}$ | 1.8   |
| $K_{\hat{v} v}$   | Half velocity constant for use of $v$ by $\hat{v}$ | 0.8   |
| $K_{\hat{w} c}$   | Half velocity constant for use of $c$ by $\hat{w}$ | 0.7   |
| $K_{\hat{w} w}$   | Half velocity constant for use of $w$ by $\hat{w}$ | 1.4   |
| $Y_{\hat{v} c}$   | Yield of $\hat{v}$ from one unit of $c$            | 1     |
| $Y_{\hat{v} v}$   | Yield of $\hat{v}$ from one unit of $v$            | 5     |
| $Y_{\hat{w} c}$   | Yield of $\hat{w}$ from one unit of $c$            | 1     |
| $Y_{\hat{w} w}$   | Yield of $\hat{w}$ from one unit of $w$            | 10    |
| $l_v$             | Production rate of $v$ by $\hat{w}$                | 0.025 |
| $l_w$             | Production rate of $w$ by $\hat{v}$                | 0.05  |
| $[c]_{\text{IN}}$ | Input concentration of carbon source               | 2     |
| $[v]_{\text{IN}}$ | Input concentration of amino acid $v$              | 0     |
| $[w]_{\text{IN}}$ | Input concentration of amino acid $w$              | 0     |

Table S2: **Parameters for the two-species auxotrophy model.** Note that values of  $l_v$ ,  $l_w$ ,  $[v]_{\text{IN}}$  and  $[w]_{\text{IN}}$  are modified in some figures. These modifications are specified in the figure caption or axes labels.

291 **4 Supplementary Figures**

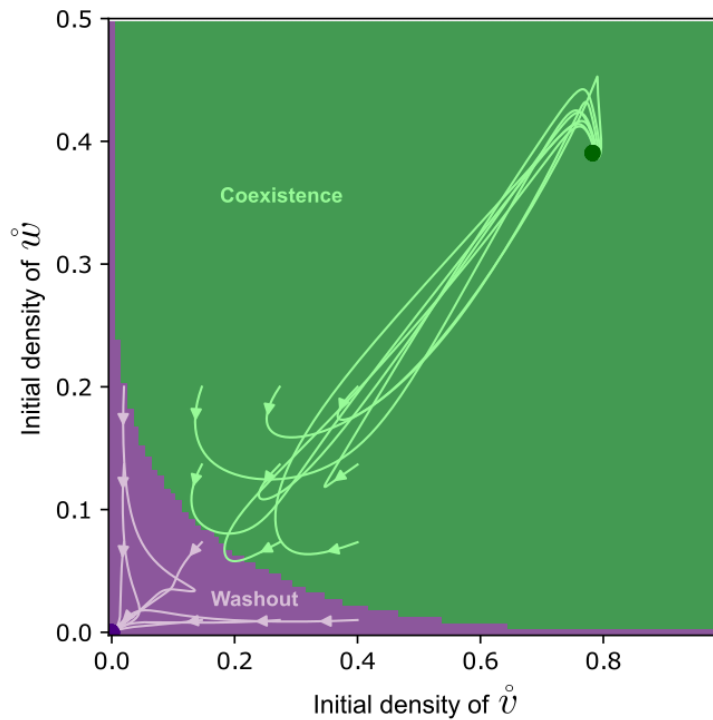


Figure S1: **Coexistence and Allee effects in the cross-feeding model.** Coloured sectors indicate basins of attraction for different starting densities for the two auxotrophs (green, mutual coexistence, purple, mutual extinction). Example trajectories converging on the two attractors (purple point and green point) are also shown. For a given starting density of one of the auxotrophs, pushing the starting density of the partner down to sufficiently low levels results in mutual extinction, an example of an Allee effect. This is a characteristic of obligate mutualisms [27]. Input media contains only the carbon source (no amino acids).  $D = 0.01$ .

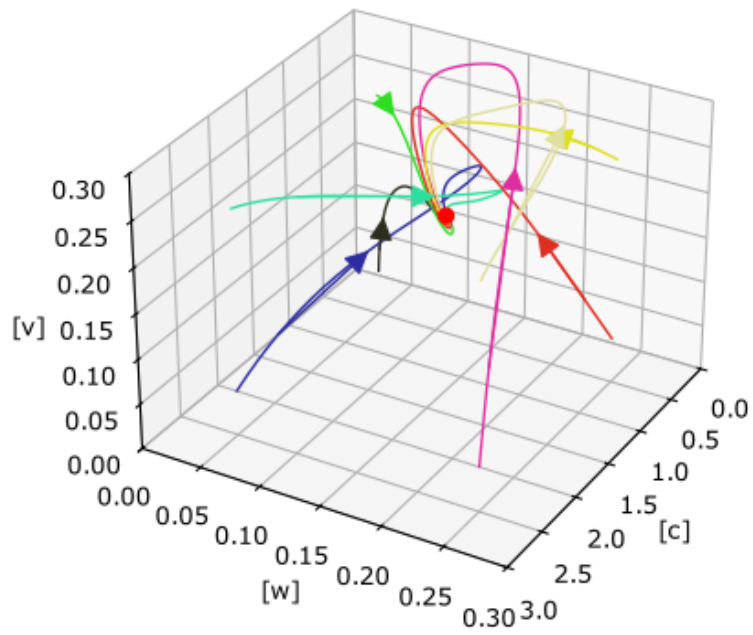


Figure S2: **The three-dimensional environment space.** Environmental trajectories for two-species chemostats initiated with varying initial compositions are plotted in different colours and converge on the equilibrium state  $r^*$  (red dot). Initial concentrations of the amino acids  $v$  and  $w$  are 0.05 or 0.25, while those of the carbon source  $c$  are 0.5 or 2.5. Input media contains only carbon at  $[c]_{\text{IN}} = 3$ .  $D = 0.01$ .

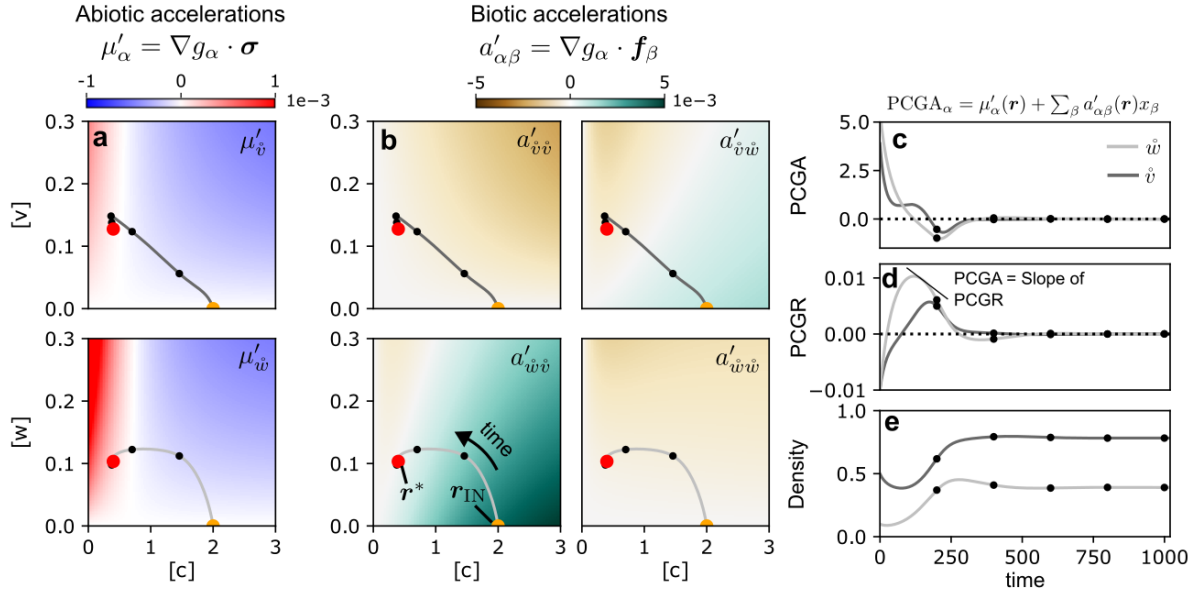


Figure S3: **The aEO equation describes ecosystem transients.** a,b) Scalar fields of the abiotic accelerations (a) and biotic accelerations (b), replicated from Fig. 2. We plot on top of these an environmental trajectory for a system initiated with the same environment as in the input media, which contains only carbon. The per-capita growth acceleration (PCGA) is determined by the aEO equation (Eq. 5), which is parameterised using the value of these scalar fields at each timepoint (c). Integration of the PCGA gives the time-varying per-capita growth rate (PCGR), which can itself be integrated to give the dynamics of the population densities (e). Black points along environmental trajectories (a,b) correspond to equally-spaced timepoints (c-e).  $D = 0.01$ .

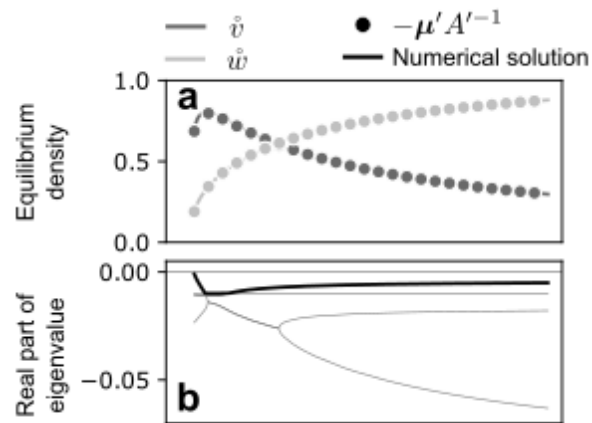


Figure S4: **Equilibrium abundances and stability analysis for amino acid production sweep.** Shown are equilibrium abundances (a) and the real part of the eigenvalue spectrum (b) (Supplementary Note 2.3.2, Fig. S5) for the set of simulations presented in Fig. 3. We also confirmed the equivalency between Eqs. 6 and 1 by using the values of the effective gLV parameters to estimate the equilibrium densities through the expression  $\mu' A'^{-1}$ , where  $\mu'$  and  $A'$  are built from the equilibrium values shown in panels a and d of Fig. 3 (a, circles).

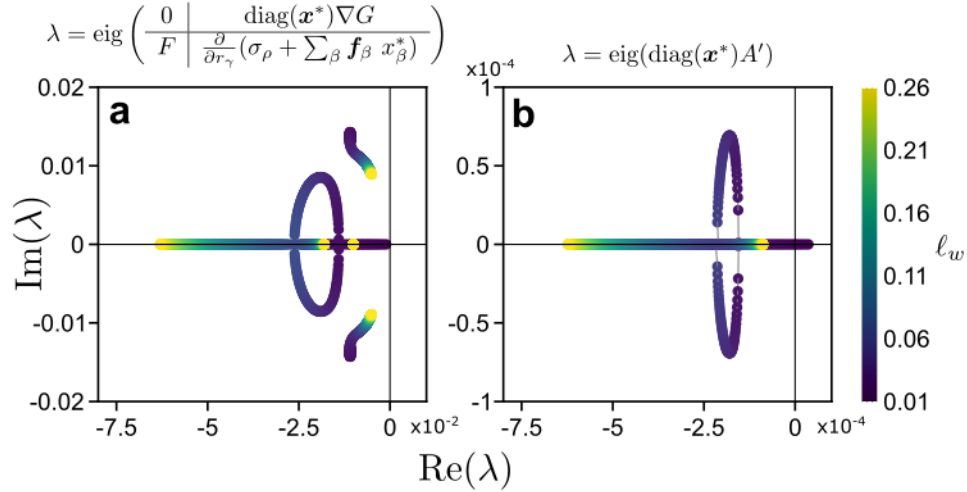


Figure S5: **Eigenvalue spectra for mechanistic models.** We show variations in the eigenvalue spectrum of the two-species auxotrophy model as the production rate of  $w$  by  $v$  ( $\ell_w$ ) is varied. In a), we show the eigenvalues of the true Jacobian matrix which includes resource dynamics (Eq. S.19). In b), we show the eigenvalues of the matrix which is the accelerational analogue of the gLV Jacobian (Eq. S.17). The simulations used to construct this figure are the same as those used in Fig. 3. Note that we show the real part of panel a in Fig. S4b.

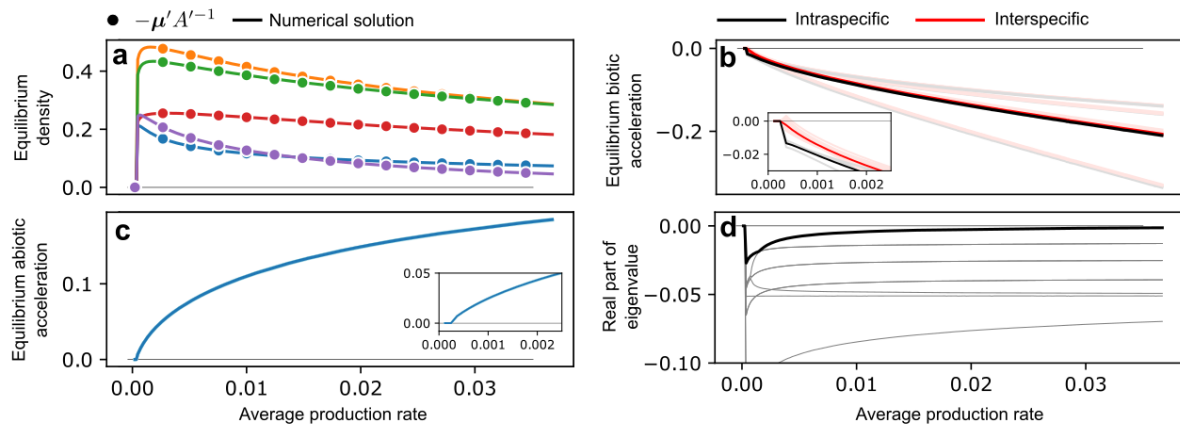


Figure S6: **5 species cross-feeding communities can be stable.** We constructed simulated communities of five auxotrophs with randomised mechanistic parameters and grew them in a chemostat on amino acid-free media (Methods). As in Fig. 3, we show the equilibrium abundances (a), biotic accelerations (b, red lines indicate interspecific values and black lines intraspecific values), abiotic accelerations (c) and real part of eigenvalue spectrum (d) for different average amino acid production rates. Insets in panels b and c show zoomed-in regions of the main plot. Black line in d indicates value of the maximal eigenvalue.

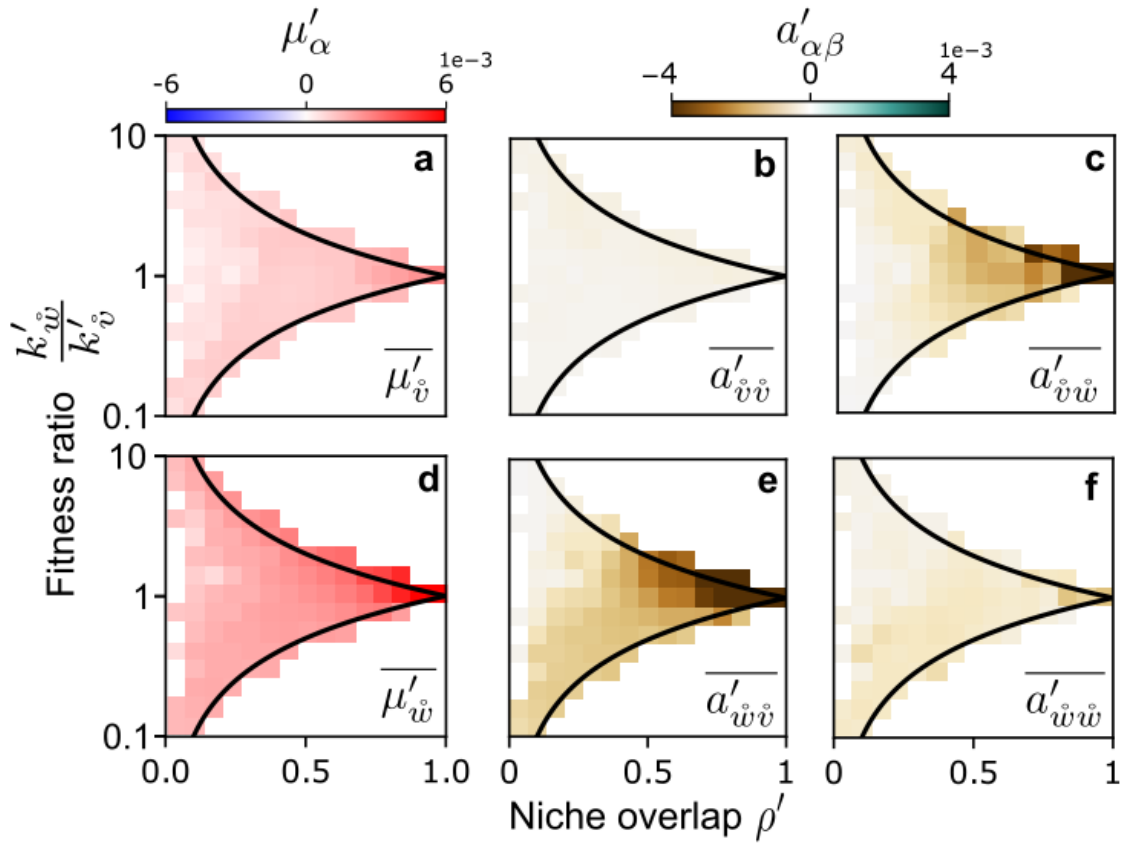


Figure S7: **Variation of effective gLV parameters on the niche overlap and relative fitness difference axes.** We display equivalent analysis as in Fig. 5a-g for the effective gLV parameters of the two species auxotrophy model. Shown are averages of abiotic accelerations (a,d) and biotic accelerations (b,c,e,f).

## References

1. Mee, M. T., Collins, J. J., Church, G. M. & Wang, H. H. Syntrophic exchange in synthetic microbial communities. *Proceedings of the National Academy of Sciences* **111**. Publisher: Proceedings of the National Academy of Sciences, E2149–E2156. <https://www.pnas.org/doi/abs/10.1073/pnas.1405641111> (2025) (May 2014).
2. Ross, T. D., Im, H., Keogh, B. G., Klausmeier, C. A. & Venturelli, O. S. Metabolic interplay drives population cycles in a cross-feeding microbial community. en. *Nature Communications* **16**. Publisher: Nature Publishing Group, 8919. ISSN: 2041-1723. <https://www.nature.com/articles/s41467-025-63986-y> (2026) (Oct. 2025).
3. Meacock, O. J. & Mitri, S. Environment-Organism Feedbacks Drive Changes in Ecological Interactions. en. *Ecology Letters* **28**. eprint: <https://onlinelibrary.wiley.com/doi/pdf/10.1111/ele.70027>, e70027. ISSN: 1461-0248. <https://onlinelibrary.wiley.com/doi/abs/10.1111/ele.70027> (2025) (2025).
4. O'Dwyer, J. P. Whence Lotka-Volterra?: Conservation laws and integrable systems in ecology. *Theoretical Ecology* **11**. Publisher: Springer Netherlands, 441–452. ISSN: 18741746. <https://link.springer.com/article/10.1007/s12080-018-0377-0> (2022) (Dec. 2018).
5. Sakarchi, J. & Germain, R. M. MacArthur's Consumer-Resource Model: A Rosetta Stone for Competitive Interactions. *The American Naturalist* **205**. Publisher: The University of Chicago Press, 306–326. ISSN: 0003-0147. <https://www.journals.uchicago.edu/doi/full/10.1086/733516> (2025) (Mar. 2025).
6. MacArthur, R. Species packing, and what competition minimizes. *Proceedings of the National Academy of Sciences* **64**. Publisher: Proceedings of the National Academy of Sciences, 1369–1371. ISSN: 0027-8424. <https://www.pnas.org/content/64/4/1369> (2021) (Dec. 1969).
7. Posfai, A., Taillefumier, T. & Wingreen, N. S. Metabolic Trade-Offs Promote Diversity in a Model Ecosystem. *Physical review letters* **118**. Publisher: NIH Public Access, 028103. ISSN: 10797114. [/pmc/articles/PMC5743855/](https://pubmed.ncbi.nlm.nih.gov/31111111/) (2022) (Jan. 2017).
8. Tilman, D. *Resource Competition and Community Structure*. ISBN: 978-0-691-08302-5. <https://www.jstor.org/stable/j.ctvx5wb72> (2026) (Princeton University Press, 1982).
9. Letten, A. D., Ke, P. J. & Fukami, T. Linking modern coexistence theory and contemporary niche theory. *Ecological Monographs* **87**. Publisher: John Wiley & Sons, Ltd, 161–177. ISSN: 1557-7015. <https://onlinelibrary.wiley.com/doi/full/10.1002/ecm.1242> (2022) (May 2017).
10. Chesson, P. MacArthur's consumer-resource model. *Theoretical Population Biology* **37**, 26–38. ISSN: 0040-5809. <https://www.sciencedirect.com/science/article/pii/S004058099090025Q> (2025) (Feb. 1990).
11. De Jesús Astacio, L. M., Prabhakara, K. H., Li, Z., Mickalide, H. & Kuehn, S. Closed microbial communities self-organize to persistently cycle carbon. *Proceedings of the National Academy of Sciences* **118**. Publisher: Proceedings of the National Academy of Sciences, e2013564118. <https://www.pnas.org/doi/abs/10.1073/pnas.2013564118> (2024) (Nov. 2021).
12. Dedrick, S., Warriar, V., Lemon, K. P. & Momeni, B. When does a Lotka-Volterra model represent microbial interactions? Insights from in vitro nasal bacterial communities. *mSystems* **8**. Publisher: American Society for Microbiology, e00757–22. <https://journals.asm.org/doi/full/10.1128/msystems.00757-22> (2025) (June 2023).
13. Liu, X., Constable, G. W. A. & Pitchford, J. W. Feasibility and stability in large Lotka Volterra systems with interaction structure. *Physical Review E* **107**. Publisher: American Physical Society, 054301. <https://link.aps.org/doi/10.1103/PhysRevE.107.054301> (2025) (May 2023).

343  
344  
345  
346  
347  
348  
349  
350  
351  
352  
353  
354  
355  
356  
357  
358  
359  
360  
361  
362  
363  
364  
365  
366  
367  
368  
369  
370  
371  
372  
373  
374  
375  
376  
377  
378  
379  
380  
381  
382  
383  
384  
385  
386  
387  
388  
389  
390  
391  
392  
393

14. Butler, S. & O'Dwyer, J. P. Stability criteria for complex microbial communities. *Nature Communications* **9**. Publisher: Nature Publishing Group, 1–10. ISSN: 2041-1723. <https://www.nature.com/articles/s41467-018-05308-z> (2022) (July 2018).
15. Liu, Y., Hu, J., Lee, H. & Gore, J. Complex Ecosystems Lose Stability When Resource Consumption Is Out of Niche. *Physical Review X* **15**. Publisher: American Physical Society, 011003. <https://link.aps.org/doi/10.1103/PhysRevX.15.011003> (2026) (Jan. 2025).
16. Gibbs, T., Levin, S. A. & Levine, J. M. Coexistence in diverse communities with higher-order interactions. *Proceedings of the National Academy of Sciences* **119**. Publisher: Proceedings of the National Academy of Sciences, e2205063119. <https://www.pnas.org/doi/full/10.1073/pnas.2205063119> (2024) (Oct. 2022).
17. Chesson, P. Mechanisms of Maintenance of Species Diversity. en. *Annual Review of Ecology, Evolution, and Systematics* **31**. Publisher: Annual Reviews, 343–366. ISSN: 1543-592X, 1545-2069. <https://www.annualreviews.org/content/journals/10.1146/annurev.ecolsys.31.1.343> (2024) (Nov. 2000).
18. Barabás, G., D'Andrea, R. & Stump, S. M. Chesson's coexistence theory. en. *Ecological Monographs* **88**. \_eprint: <https://esajournals.onlinelibrary.wiley.com/doi/pdf/10.1002/ecm.1302>, 277–303. ISSN: 1557-7015. <https://onlinelibrary.wiley.com/doi/abs/10.1002/ecm.1302> (2025) (2018).
19. Saavedra, S. et al. A structural approach for understanding multispecies coexistence. en. *Ecological Monographs* **87**. \_eprint: <https://esajournals.onlinelibrary.wiley.com/doi/pdf/10.1002/ecm.1263>, 470–486. ISSN: 1557-7015. <https://onlinelibrary.wiley.com/doi/abs/10.1002/ecm.1263> (2025) (2017).
20. Spaak, J. W. & De Laender, F. Intuitive and broadly applicable definitions of niche and fitness differences. en. *Ecology Letters* **23**. \_eprint: <https://onlinelibrary.wiley.com/doi/pdf/10.1111/ele.13511>, 1117–1128. ISSN: 1461-0248. <https://onlinelibrary.wiley.com/doi/abs/10.1111/ele.13511> (2025) (2020).
21. Koffel, T., Daufresne, T. & Klausmeier, C. A. From competition to facilitation and mutualism: a general theory of the niche. *Ecological Monographs* **91**. Publisher: John Wiley & Sons, Ltd, e01458. ISSN: 1557-7015. <https://onlinelibrary.wiley.com/doi/full/10.1002/ecm.1458> (2023) (Aug. 2021).
22. Song, C., Barabás, G. & Saavedra, S. On the Consequences of the Interdependence of Stabilizing and Equalizing Mechanisms. *The American Naturalist* **194**. Publisher: The University of Chicago Press, 627–639. ISSN: 0003-0147. <https://www.journals.uchicago.edu/doi/full/10.1086/705347> (2024) (Nov. 2019).
23. Orr, J. A., Armitage, D. W. & Letten, A. D. Coexistence Theory for Microbial Ecology, and Vice Versa. en. *Environmental Microbiology* **27**. Publisher: John Wiley & Sons, Ltd, e70072. ISSN: 1462-2920. <https://enviromicro-journals.onlinelibrary.wiley.com/doi/10.1111/1462-2920.70072> (2026) (Mar. 2025).
24. Kelsic, E. D., Zhao, J., Vetsigian, K. & Kishony, R. Counteraction of antibiotic production and degradation stabilizes microbial communities. *Nature* **521**. Publisher: Nature Publishing Group, a division of Macmillan Publishers Limited. All Rights Reserved., 516–519. ISSN: 0028-0836. <http://dx.doi.org/10.1038/nature14485> (2015) (May 2015).
25. Goldford, J. E. et al. Emergent simplicity in microbial community assembly. *Science* **361**. Publisher: American Association for the Advancement of Science, 469–474. ISSN: 10959203. <http://science.sciencemag.org/> (2021) (Aug. 2018).
26. Niehaus, L. et al. Microbial coexistence through chemical-mediated interactions. *Nature Communications* **10**. Publisher: Nature Publishing Group, 1–12. ISSN: 2041-1723. <https://www.nature.com/articles/s41467-019-10062-x> (2022) (May 2019).
27. Hale, K. R. S. & Valdovinos, F. S. Ecological theory of mutualism: Robust patterns of stability and thresholds in two-species population models. en. *Ecology and Evolution* **11**. \_eprint:

394

<https://onlinelibrary.wiley.com/doi/pdf/10.1002/ece3.8453>, 17651–17671. ISSN: 2045-7758.

395

<https://onlinelibrary.wiley.com/doi/abs/10.1002/ece3.8453> (2026) (2021).